Submitted to the Journal of Chemical Physics, *June 23, 2003*

The Role of Electronic Symmetry in Charge-Transfer-to-Solvent (CTTS) Reactions: Quantum Non-Adiabatic Computer Simulation of Photoexcited Sodium Anions

C. Jay Smallwood, Wayne B. Bosma,[†] Ross E. Larsen and Benjamin J. Schwartz*

Department of Chemistry and Biochemistry
University of California, Los Angeles
Los Angeles, CA 90095-1569

*author to whom correspondence should be addressed: e-mail: **schwartz@chem.ucla.edu**
voice: (310) 206-4113; fax: (310) 206-4038

[†]Department of Chemistry, Bradley University, Peoria, IL 61625

Abstract: In charge-transfer-to-solvent (CTTS) reactions, photoexcitation of a solute produces an excited state in which the excited electron is not bound directly to the solute, but is instead localized by the polarization of the solvent molecules surrounding the solute. Such solvent-supported CTTS excited states are short-lived: the solvent motions that respond to the excitation push the excited electron out of the solute's cavity, producing a solvated solute with one less charge and a solvated electron. Since CTTS represents the simplest possible solvent-driven electron transfer reaction, there has been considerable interest in understanding the solvent motions responsible for electron ejection. To date, most of the theoretical attention on CTTS has focused on the aqueous halides, in which the ground state has the electron in a *p* orbital so that the one-photon-allowed solvent-supported CTTS excited state has *s*-like symmetry. The question we explore in this paper is what role the symmetry of the electronic states plays in determining the solvent motions that account for CTTS. To this end, we have performed a series of one-electron mixed quantum/classical non-adiabatic molecular dynamics simulations of the CTTS dynamics of sodide, Na^-, which has its

ground-state electron in an *s* orbital and solvent-supported CTTS excited states of *p*-like symmetry. In fact, the electronic structure of Na^- is quite similar to that of the hydrated electron, the only difference being that Na^- has a sodium atom functioning both to hold open the cavity in the solvent and to stabilize the electronic wave functions. We have chosen to simulate the CTTS dynamics of Na^- in water (even though the Na^-/water system does not exist experimentally) to make direct comparisons with previous theoretical work on both the CTTS reaction of the aqueous halides and the relaxation dynamics of the hydrated electron. Like the photoexcited hydrated electron, we find that the key motions for relaxation involve translations of solvent molecules into the node of the *p*-like solvent-supported CTTS excited state of sodide. Unlike the hydrated electron, this solvation of the electronic node leads to migration of the excited CTTS electron, leaving one of the *p*-like lobes pinned to the sodium atom core and the other extended into the solvent; this nodal migration causes a breakdown of linear response. We also investigate the non-adiabatic transition out of the CTTS excited state and the subsequent return to equilibrium, and we find dramatic differences between the relaxation dynamics of sodide and the halides that result directly from differences in electronic symmetry. Since the ground state of the ejected electron is *s*-like, detachment from the *s*-like CTTS excited state of the halides occurs directly, but detachment cannot occur from the *p*-like CTTS excited state of Na^- without a non-adiabatic transition to remove the node. Thus, unlike the halides, CTTS electron detachment from sodide occurs only after relaxation to the ground state and is a relatively rare event. All the results are compared to experimental work on Na^- CTTS dynamics in non-aqueous solvents, and a unified picture for the electronic relaxation of solvent-supported excited states for any symmetry is presented.

I. Introduction

The effects of solvation on condensed-phase reactions have long been an area of active research. Since condensed phase environments can be very complex, simple systems with limited reactive pathways are needed to provide detailed insight into the role of solvation in condensed-phase reactivity. Thus, there has been an increasing amount of research into the simplest class of solution-phase charge transfer reactions, charge-transfer-to-solvent (CTTS) systems.[1] CTTS transitions result from additional bound states for an ionizable electron that are introduced by solvent stabilization. Upon photoexcitation from the ground state to a higher energy solvent-supported state, delayed electron detachment is often observed. Since the solvent is solely responsible for these transitions, CTTS systems provide insight into the manner in which solvent motions control electron transfer.

Though the seminal work on CTTS systems began decades ago[1], there has been a recent revival of interest in CTTS reactions arising from the ability to examine dynamics on sub-picosecond timescales with ultrafast lasers.[2–5] The aqueous halides have been the subject of most of the attention, providing insight into the motions of arguably the most important solvent, water. In addition to experiments, concurrent advances in computational technology have allowed for large-scale calculations of CTTS dynamics.[6–11] For example, simulations by Sheu and Rossky of photoexcited aqueous iodide have provided a molecular-level picture of the CTTS electron detachment process.[6–8] These calculations used a one-electron model of iodide that allowed for non-adiabatic transitions between eigenstates. The equilibrium electronic structure was characterized by a *p*-like ground state, a band of six CTTS states of mixed *s* and *d* symmetry, and three higher-energy *p*-like states, all of which were contained within solvent cavity around the ion. The simulations,

which modeled the two-photon excitation used in experiments by Eisenthal and co-workers,[4] showed two mechanisms for electron detachment: a direct detachment pathway and a delayed CTTS detachment pathway.[6–8]

More recent experiments by Bradforth and co-workers have explored the dynamics following direct one-photon excitation into the CTTS band of aqueous iodide, and found rapid formation of detached solvated electrons.[2] The simulations of Sheu and Rossky,[6–8] as well as similar calculations for aqueous chloride by Staib and Borgis,[9] suggest that for one-photon excitation, only the direct detachment pathway is accessible. Once the electron is in the lowest solvent-supported excited state, the simulations found rapid (< 20 fs) detachment in every run, followed by recombination on longer time scales, in good agreement with Bradforth and co-workers' one-photon experiments. The simulations also predict a unit detachment probability, in agreement with recent reports[12] that have challenged earlier measurements.[13]

Although the theoretical results for CTTS discussed above are in good general agreement with experiment, they all have relied on one-electron, mixed quantum/classical MD simulations in which multi-electron effects such as exchange are not taken into account. Recent calculations by Jungwirth and Bradforth[10] using static quantum chemical methods to calculate the electronic structure of aqueous iodide found only a single CTTS excited state instead of the 6 states of mixed *s*-and-*d* symmetry observed in the one-electron simulations by Sheu and Rossky.[6-8] Jungwirth and Bradforth have argued that the neglect of exchange in the one-electron simulations artificially lowers the energy of the *d*-like solvent-supported orbitals. However, since the CTTS detachment process was found to proceed only though the lowest CTTS state in the one-electron simulations,[6–8] it is not clear whether neglect of multi-electron effects has an important impact on the calculated

detachment dynamics; simulation of multi-electron CTTS dynamics only now becoming computationally feasible.[14] Yet, the one-electron simulations' qualitative agreement with experiment suggests that while certainly not ideal, one-electron models can accurately represent the principal features of CTTS detachment.

In addition to the halides, another CTTS system that has been the focus of recent experimental work is the alkali metal anion sodide, Na^-.[15–17] Although sodide cannot be prepared in water and must be studied in aprotic solvents such as tetrohydrofuran (THF), the CTTS transition(s) of Na^- are in the visible and near IR, making the experiment spectroscopically convenient. The CTTS dynamics of Na^- are similar in many ways to those of the aqueous halides, but there are several important differences, such as a dependence of the detachment dynamics on the excitation energy in sodide[15] but not in iodide.[2] What could cause such differences? One possibility is that the differences arise from the change in electronic symmetry between the halides and sodide: Na^- has an *s*-like ground state, in contrast to the *p*-like ground state of the halides. Thus, it would not be surprising to find that the reversed symmetry of Na^- plays an important role when comparing the two systems.

Na^- has the same electronic symmetry as the hydrated electron, which has itself been the focus of numerous experimental[18] and theoretical studies.[19–22] In most calculations, the hydrated electron exists within a solvent cavity and has an electronic structure like that of a particle in a finite spherical box, with an *s*-like ground state and three *p*-like excited states. In fact, the only difference between the hydrated electron and Na^- is the presence of the attractive sodium atomic core in the case of Na^-. Therefore, a simulation study of Na^- can provide a connection between the previous theoretical studies of the aqueous halides and the hydrated electron. In addition to addressing the

role of electronic symmetry in CTTS reactions, a theoretical study of sodide will allow us to examine the effects of the presence of an attractive atomic core on the dynamics of both electronic and solvent relaxation.

In this paper, we present the first in a series of theoretical studies to ascertain the similarities and differences between sodide and other CTTS systems, with the ultimate goal of providing a direct comparison with the Na^- experiments.[15-17] In particular, we examine how the wave function symmetry of sodide controls the response of the solvent to direct one-photon excitation into the CTTS band. In order to make comparisons with the previous calculations of both iodide[6–8] and the hydrated electron,[19-22] we have chosen to use water as the solvent. Although the Na^-/water system is not experimentally accessible, our choice of water is not as drastic as it would seem. The reason that the Na^-/water system is experimentally unstable is due to the strong potential of sodide to reduce water, but this reaction pathway does not exist in our simulations because the O-H bonds of the simulated water cannot break. Thus, not only are we able to make direct comparisons with previous work on the aqueous halides and hydrated electron, but our calculations provide a limiting case of the CTTS solvation mechanism of sodide in an aprotic solvent that is faster and more polar than THF. Hence, this study also will provide a qualitative glimpse into the molecular details of the solvent response to CTTS photoexcitation for the Na^-/THF experiments.

In the following, we present a set of mixed quantum/classical non-adiabatic one-electron trajectories that simulate one-photon CTTS excitation of a sodide-like solute in liquid water. In Section II, we outline our methodology. Then, in Section III, we present the equilibrium electronic structure of simulated aqueous Na^- as well as the non-adiabatic trajectories resulting from excitation to the CTTS band. In Section IV, we discuss the solvent response following CTTS excitation and

make a detailed comparison to previous simulations of both CTTS and the hydrated electron. We conclude with general remarks concerning CTTS and the nature of electronic relaxation in liquids in Section V.

II. Computational Methodology

Due to the strong coupling between motions of the solvent and the electronic energies of our quantum Na^- solute, our simulations require use of a non-adiabatic methodology; we have chosen the mean-field-with-surface-hopping (MF/SH) algorithm of Prezhdo and Rossky[23] for these calculations. This method is essentially an amalgam of mean-field dynamics[24] and the Tully fewest-switches surface-hopping method.[25] Although the MF/SH methodology has not been as widely used as the molecular dynamics with electronic transitions (MDET) method of Tully[25] or the stationary-phase surface-hopping (SPSH) method of Webster *et al.*,[26,27] MF/SH has several advantages over MDET and SPSH. Like other mean-field methods, MF/SH allows not only for the existence of a superposition of basis states in regions of strong non-adiabatic coupling, but also includes surface hopping to ensure the correct asymptotic behavior in regions of low coupling. One consequence of this is that MF/SH seems to be less sensitive to the choice of basis representation than other non-adiabatic methodologies.[23] This is important for our simulations since there is no natural diabatic basis set for the Na^- CTTS reaction. Recent calculations by Wong and Rossky have demonstrated the viability of MF/SH for high dimensional, strongly coupled systems, such as the hydrated electron.[19] Our computational implementation is a direct offspring of the hydrated electron calculations of Wong and Rossky and is described in detail in reference 19. Here, we discuss the specifics of our implementation and comment on the method only as it relates to our calculations.

To simulate the response of sodide to one-photon excitation into the CTTS band, we ran 54 non-equilibrium, non-adiabatic mixed quantum/classical MF/SH molecular dynamics trajectories. The quantum degree of freedom was a single electron immersed in a classical bath consisting of 200 water molecules and a neutral sodium atom. For each non-equilibrium run, we simulated one-photon excitation by switching the electron into the appropriate excited state, chosen when the ground-to-excited-state energy gap was within ±0.01 eV of the energy corresponding to the maximum of the first band in the equilibrium distribution of ground-to-excited state energy gaps (see Fig. 2, below). The excited-state trajectories were run until the electron relaxed to the ground state and returned to equilibrium. Following 18 ps of equilibration, initial configurations for the excited-state runs were chosen from a 72-ps equilibrium run. Each initial configuration is separated from the previous one by at least 1 ps; thus the starting configurations for the excited-state runs should be statistically independent. Since our calculations show that the oscillator strengths for excitation to each of the three CTTS states are roughly equal, the one-photon excited trajectories were weighted equally in all non-equilibrium ensemble averages.

In the MF/SH algorithm, the electronic eigenstates are computed at every time step. The eigenstates are completely determined by pseudopotentials representing the interaction of the electron with both the solvent molecules and the Na atom. The electron-water pseudopotential we chose was developed by Schnitker and Rossky,[28] allowing us to make direct comparisons with previous simulations of both iodide[6–8] and the hydrated electron[19-21] from the Rossky group. This pseudopotential contains three terms representing electrostatic, polarization, and Pauli repulsion contributions.[28] Following earlier simulations of iodide,[6–8] we modeled the Na-electron contribution as a modified Heine-Abarenkov pseudopotential,[29]

$$V(r) = \begin{cases} V_0 & r < r_0 \\ V_{outer} & r \geq r_0 \end{cases} \tag{1}$$

Inside the cutoff radius, r_o, the potential is chosen to be constant, representing a balance of the exchange and electrostatic interactions.[30] Outside r_o, there is a Coloumbic potential for a neutral sodium atom with a $+11e$ charged nucleus and 11 electrons described by appropriate Slater orbitals.[31] Thus,

$$V_{outer}(r) = \frac{-e^2}{r}\sum_{n=1}^{3} g_n e^{-a_n r}\sum_{k=1}^{2n}(1-\tfrac{k}{2n})\frac{(a_n r)^k}{k!}, \tag{2}$$

where g_n is the number of electrons and a_n is the appropriate parameter for a given Slater orbital. When continuity of the total potential is enforced, there is only one free parameter. We chose this to be the cutoff radius, and set r_o = 1.25 Å in order to match the known electron affinity of 0.55 eV for gas-phase sodium.[32] To verify the accuracy of this approach, we also derived a one-electron pseudopotential for neutral sodium, fixing the cutoff radius so as to match the ionization potential. The resulting pseudopotential gives the energy of the sodium D-line to within 4.1%.

For each solvent configuration, the lowest six adiabatic eigenstates were determined using an iterative block-Lanczos technique that is particularly effective for finding the lowest-energy bound eigenvectors of complicated potentials.[26] This technique uses a discrete cubic grid of points and finds the value of the eigenfunctions at each point. For our calculations, we chose a 16^3 grid with length 18.17 Å on a side. This grid, which was the same size as the simulation box, was sufficiently dense as to provide accurate wave functions, satisfying $H|\psi\rangle = E|\psi\rangle$ within at least 10 μeV. We ran several trajectories using a 32^3 grid and found no quantitative difference in the dynamics. In addition, use of a larger number of eigenstates did not alter the observed dynamics.

At each time step, the MF/SH algorithm evaluates whether there is sufficient coupling between states to allow a non-adiabatic transition. The non-adiabatic coupling between two electronic states is given by $\dot{\boldsymbol{R}} \cdot \boldsymbol{d}_{ij}$, with,

$$\boldsymbol{d}_{ij} = \left\langle \phi_i(r;\boldsymbol{R}) \middle| \nabla_{\boldsymbol{R}} \phi_j(r;\boldsymbol{R}) \right\rangle \tag{3a}$$

where the dot product includes a sum over all classical degrees of freedom. If the electronic states are adiabatic eigenstates then $\boldsymbol{d}_{ij}$ can be written as,[33]

$$\boldsymbol{d}_{ij} = \frac{\langle \phi_i | \nabla_{\boldsymbol{R}} H | \phi_j \rangle}{|E_j - E_i|} \tag{3b}$$

where the differentiation is with respect to the classical nuclear coordinates, $\boldsymbol{R}$. MF/SH uses two parallel trajectories to evaluate the transition probabilities. Furthermore, MF/SH also checks to ensure that mean-field consistency criteria are not violated. These criteria arise from the requirement that the classical trajectories resulting from the parallel quantum paths are not overly divergent, as discussed in detail in Ref 23.

Once the eigenstates for an instantaneous (water and sodium) configuration are determined, the classical particles are propagated forward in time. The solvent is represented by the SPC/Flexible model of water.[34] The classical interactions between the neutral sodium atom and the solvent are treated using a Lennard-Jones potential. We determined the Na–O Lennard-Jones well depth, ε = 1.597 kJ/mol, using the Lorenz-Berthelot combining rules[35] employing a Na–Na interaction calculated by Chekmarev et al;[36] we also verified that the dynamics were robust to changes in the Na–O Lennard-Jones well depth. The Lennard-Jones Na–O diameter was determined as σ = 3.22 Å using the combining rules with the Na-Na distance given in Ref. 36 and O–O

distances used in the SPC/ Flexible model.

The forces exerted by the quantum wave function on the classical particles are given by the Hellman-Feynman theorem.[37] These forces, combined with the classical forces from the bath molecules and the sodium atom, are used to propagate the classical particles using the velocity-Verlet algorithm with a 0.5-fs time step. The simulation box size was chosen so that the density was 0.997 g/cm^3, and cubic periodic boundary conditions were employed. These constant *N*, *V*, and *E* trajectories had temperatures of 313 ± 7 K.

Before discussing the dynamics observed in the simulations, we wish to make one final comment on our choice to use a one-electron method. One potential objection to the use of one-electron mixed quantum/classical simulations in studying CTTS and solvated electron dynamics is the lack of quantum mechanical treatment of the solvent. This objection has been used to question the cavity model of the hydrated electron, with a few researchers proposing that electron transfer to the frontier orbitals of the solvent is more important than cavity formation for electron solvation.[38] Though it seems reasonable that there will be some transfer to the solvent orbitals that cannot be accounted for in one-electron simulations, the static calculations of the iodide CTTS states by Jungwirth and Bradforth, in which the first solvent shell was treated quantum mechanically, found a minimal amount of electron transfer into the solvent frontier MOs.[10] The ample agreement between experiment[2,4,18] and one-electron simulations[6-8,19–22] provides strong support for the use of one-electron models and the physical insight that they provide.

III. Results

A. The Equilibrium Electronic Structure of Aqueous Na^-

To understand the non-adiabatic dynamics, we must first discuss the equilibrium electronic structure of condensed-phase sodide. A representative 1-ps portion of the equilibrium trajectory is shown in Figure 1. There are four bound states, an *s*-like ground state and three *p*-like excited states of split degeneracy due to asymmetry in the local solvent environment. Above these is a continuum of unbound states; we calculated only two of these continuum states in our simulations because they did not play an important role in the dynamics. Since both model calculations and experiments[32] show that there exists only one bound state in gas-phase sodide with ~0.55-eV binding energy, the electronic structure in Fig. 1 illustrates the pivotal role of the solvent in providing additional stabilization for the electronic wave functions. This manifold of solvent-supported states is similar to that seen in other CTTS systems[6-9] as well as the hydrated electron.[19-22] The equilibrium density of states (DOS) of our model of aqueous sodide is summarized in Figure 2. There is an energy spacing of roughly 0.3 eV between the centers of the consecutive *p*-like bands. While the peaks in the DOS are sharp, there are a number of configurations in which the second and third *p*-like states lie at the energy of the maximum of the first DOS peak. This means that excitation of the CTTS electron with an energy corresponding to the peak of the energy gap distribution between the ground and first excited states, indicated by the arrow in the figure, also results in excitations to higher-lying excited states.

Figures 1 and 2 also make clear that general electronic structure of Na^- is very similar to that of the hydrated electron. This is as expected, since both Na^- and the hydrated electron have the same (solvent-perturbed) symmetry, with an *s*-like ground state and 3 solvent-supported *p*-like

states. However, the bound states of sodide are lower in energy than those of the hydrated electron due to the attractive nature of the Na core potential (Eq. 2). Furthermore, the core potential serves to increase the ground-to-excited state energy gap of Na^- relative to the solvated electron because the ground state of Na^- has more (radial) overlap with the attractive core potential than do the *p*-like excited states. Consistent with other CTTS[6-9] and hydrated electron[19-22] simulations, the fluctuations of the quantum energy levels are large, illustrating the sensitivity of the quantum subsystem to motions of the solvent.

B. Non-adiabatic Trajectories Following One-Photon CTTS Excitation

We now discuss the features of 54 non-adiabatic trajectories where, for each run, the ground state was excited to a state 4.4 eV above the ground state energy. We begin by examining the lifetime of the excited electron. Figure 3 shows the survival probability for the electron to remain in the excited state as a function of time. It is clear that the sodide system has a dramatically different distribution of lifetimes than the hydrated electron: For the hydrated electron, the average lifetime was 730 fs and the shortest lifetime was 35 fs.[20] For sodide, the average excited-state lifetime is 1210 fs with a median of 1070 fs, and none of the trajectories relax to the ground state before 400 fs. This disparity illustrates the importance of the core in controlling the non-adiabatic coupling between the ground and excited states. In fact, 93% of the Na^- trajectories remain in the excited state after 500 fs. After this initial plateau, the survival probability decays roughly exponentially as trajectories make the non-adiabatic transition to the ground state. As we will argue below, the delayed onset of non-adiabatic relaxation results from the time it takes the solvent to close the ground-to-excited-state energy gap.

For our non-adiabatic trajectories, we found four qualitatively different types of relaxation behavior following excitation; representative trajectories illustrating each of the behaviors are shown in Figures 4-7. In each figure, Panel A plots the lowest six eigenstates as a function of time, with the occupied state shown as a bold line. All four of these figures show a brief period of time with the quantum system in the electronic ground state, before the ground-to-excited-state energy gap became resonant with the excitation energy. Panel B of the figures shows the distance between the sodium atom and the center of mass of the electron ($Na\text{-}e^-_{com}$) as a function of time for selected adiabatic eigenstates, where again the data for the occupied state is shown in bold. Panel C shows the behavior of an overlap parameter, Z, which we define as,

$$Z \equiv \int_0^{r_c} |\psi(\boldsymbol{r})|^2 d\boldsymbol{r} \tag{4}$$

i.e., the fraction of electron density contained within a given distance r_c of the sodium atom. This parameter provides us with a quantitative assessment of the extent of detachment of the electron from the sodium. We chose the overlap parameter radius to be r_c = 2.8 Å as this provided the clearest distinction between configurations in which the electron was attached or detached; we define detachment as when Z is less than 0.02 for 10 fs or longer. Panel D plots the ratio of the largest to the smallest moment of inertia of the occupied eigenstate as a function of time. This ratio, I_{max}/I_{min}, found by diagonalizing the moment of inertia tensor of the occupied-state electronic density and dividing the largest moment by the smallest moment at each time step, provides a measure of the general shape of the wave function: the ratio will be unity if the wave function is spherical and will grow larger as it becomes increasingly ellipsoidal.

We will divide our discussion of the non-equilibrium trajectories into two parts: the system

response after the initial excitation, and the behavior of the system after the non-adiabatic transition from the excited state to the ground state.

III.B.1. CTTS Dynamics in the Excited State: While there are clear qualitative differences in the long-time behavior of the representative trajectories shown in Figs. 4-7, the initial dynamics for all 54 runs are essentially the same. Excitation results in occupation of one of the three *p*-like states. The solvent, now out of equilibrium, moves to solvate the excited-state electron density; these motions also destabilize the two other *p*-like states in the CTTS band. More dramatically, these same solvent motions result in a reduction of the solvent stabilization of the now aspherical ground state. The resulting Stokes shift of the energy gap is enormous, and is similar to what is seen in excited-state simulations of both iodide CTTS[6-8] and the hydrated electron.[20] The continuum states are barely affected by the solvent motions resulting from excitation, as expected due to their diffuse nature. The large changes that occur in the electronic structure after excitation further illustrate the sensitivity of CTTS systems to solvent motions.

As suggested by the density of states (Fig. 2), several (~24%) of the runs were excited to a state above the first excited state, with the vast majority of these higher excitations going to the second excited state. Each of these higher-excited-state trajectories rapidly relaxes to the lowest excited state; this cascade to the lowest-excited eigenstate is best thought of as a series of diabatic curve crossings, since the unoccupied *p*-like states are increasing in energy relative to the occupied state. After relaxation to the lowest excited state, the solvent response continues as before, leaving no discernable difference between these higher-excited trajectories and those directly excited to the lowest excited state.[39]

Panel B in Figs. 4-7 shows that soon after excitation, the electronic center of mass, which

corresponds roughly to the node of the *p*-like CTTS excited state, moves off of the parent atom and into the solvent. This leaves one lobe of the *p*-like excited-state wave function pinned to the sodium core and the other extended out into the solvent. This *nodal migration* occurs in all of our excited-state trajectories, though not to equal extent, as quantified by the overlap parameter in Panel C of Figures 4-7. Upon excitation, the amount of charge overlapping the sodium immediately decreases as a result of the increased size of the excited wave function relative to the ground state. Then, as the excited-state wave function moves off into the solvent, the overlap parameter decreases further due to nodal migration. We believe that the driving force for this migration is interference of the sodium core with the most stabilizing solvent motions. Previous simulations of the hydrated electron found that solvation resulted from water molecules moving into the node of the excited *p*-like wave function.[20] If the *p*-like CTTS excited state of sodide remained centered on the atom, the solvent could not move into the nodal region because of repulsive interactions with the Na atom core. However, if the wave function migrates, the solvent will be able to move into the node, allowing for better solvation of the excited-state wave function. This migration occurs in an energetic competition with maintaining wave function overlap with the attractive potential of the Na core.

Figures 4-7 also show that the solvent motions that stabilize the excited state also cause the narrowing of the ground-to-excited-state energy gap. After the gap closure (and nodal migration) has occurred, the ground-state energy fluctuates around a distinct average value in each trajectory. Although the energy gap for each trajectory was different, we found no correlation between the magnitude of the gap and the system dynamics. Surprisingly, we also observed no direct correlation between the magnitude of the equilibrated-excited-state energy gap and the excited-state lifetime,

implying that the energy gap alone does not determine the non-adiabatic relaxation rate, as has been suggested for the hydrated electron.[20] The long residence times of the trajectories in the excited state indicate that once the solvent has rearranged to accommodate the excited state, the solvated excited state is metastable.

For a more quantitative measure of the stability of the nodally-migrated excited CTTS electron, we calculated the potential of mean force (PMF) between the Na atom and the excited electron, shown in Figure 8. Since the electron is a quantum mechanical object, we used the Na-electron-center-of-mass coordinate to define the distance between the two objects in the excited state. We then determined the PMF, $W(r)$, using the reversible work theorem,[40,41] which states,

$$g(r) = P(r) = e^{-\beta W_{lin}(r)} \tag{5a}$$

$$g(r) = \frac{P(r)}{4\pi r^2} = e^{-\beta W_{sph}(r)} \tag{5b}$$

where $P(r)$ is the probability distribution for finding the e^-_{com} a distance r from the Na atom (calculated by binning the Na–e^-_{com} distances) and $g(r)$ is the radial distribution function. To determine the quasi-equilibrated excited state $g(r)$, we sampled over all configurations in the excited-state trajectories that were more than 900 fs after the excitation since the average solvent response (discussed further in Section IV.C) was more than 80% complete after this time.[42] However, it is not immediately clear what form of $g(r)$ to use for the excited state Na-e^-_{com} distance. The cavity that is created by the lobe extending into the solvent does not explore the entire 4π steradians around the Na atom during the excited-state lifetime. In fact, the Na-e^-_{com} orientation remains approximately along a line in space. Thus, in Figure 8 we plot the two limiting cases of our Na-e^-_{com} distance probability distribution: where the distribution remains along a line (Fig. 8a, from

Eq. 5a) and where the excited state has explored the entire configurational surface (Fig. 8b, from Eq. 5b). Figure 8a shows that there is a well-defined geometry for the equilibrated CTTS excited-state wave function, as seen by the several-kT deep minimum in the PMF at a Na-e^-_{com} distance of ~4 Å. The PMF minimum is very broad due to the fact that the electron is a quantum-deformable object, with its center of mass fluctuating in response to small motions of the surrounding solvent molecules. Despite this breadth, this minimum shows that the *p*-like CTTS excited state with one lobe on the sodium and the other extended out into the solvent is metastable, even after the Stokes shift is largely complete. Figure 8b suggests that while there is still exists a barrier to escape, there is no free energy barrier associated with reattachment. Since our excited state explores some small-angle cone, the 'true' PMF should fall somewhere between those depicted in Figures 8a and 8b, leading us to expect that we have a metastable excited state similar to that shown in Figure 8a, but with a shallower minimum.

Although the overlap parameter and the Na–e^-_{com} distance indicate that the solvent causes the electron to extend into the solvent, presumably allowing water molecules to move into the node to create a metastable excited state, we have yet to explicitly analyze the solvent motions involved in this process. Thus, to better visualize the non-equilibrium solvent motions, we show radial distribution functions for the equilibrium ground and excited states in Figures 9 and 10, respectively, where we have plotted both the Na–H/Na–O and the e^-_{com}–H/e^-_{com}–O pair distributions. The equilibrium solvent structure is as expected for a small anion in water: the H atoms point in toward the solute, with the maximum of the first-shell Na-H $g(r)$ at 2.2 Å and the peak of the first solvent shell for O atoms lying roughly 3.2 Å from the Na core. Moreover, the equilibrium pair distributions referenced to the Na core and to the electron center of mass are nearly identical, as

expected for an electron with its spherical ground state centered on the sodium atom. Upon excitation and solvent relaxation, Figures 9 and 10 indicate that water molecules move into in the node, in agreement with our arguments above. The lack of structure in the electron-based excited-state radial distribution functions results from the use of a radial average for a non-spherical wave function.[20] The Na–O and Na–H $g(r)$'s in the figures verify that the first solvent shell is farther away after excitation, consistent with an overall size change. Perhaps most importantly, it is evident from Figures 9 and 10 that the CTTS excited-state solvation structure is not ideal for the ground-state solvation of Na^-.

III.B.2: Dynamics Following the Excited-to-Ground-State Non-adiabatic Transition: Our simulations have shown that even after the excited-state solvation dynamics are complete, the electron tends to remain in the excited state. But eventually, solvent fluctuations will sufficiently couple the ground and excited states to allow a non-adiabatic transition to the ground state. It is only after this transition to the ground state that the behaviors of the individual trajectories noticeably deviate from each other. We observe that the transition to the ground state occurs along two principal pathways: either the electron remains bound to the sodium core at all times after the transition, or it detaches from the core for a period of time. With this definition, we have classified our trajectories into four different types based on their behavior after non-adiabatic relaxation: non-detachment with immediate relaxation, non-detachment with delayed relaxation, short-lifetime electron detachment, and long-lifetime electron detachment.

***Non-detachment with Immediate Relaxation*:** In this most common pathway, illustrated in Fig. 4, which occurs in more than half (56%) of the trajectories, there is a rapid relaxation back to the

equilibrium ground state immediately after the non-adiabatic transition. The plot of I_{max}/I_{min} in Fig. 4C shows that the wave function rapidly becomes spherical after the transition to the ground state. The wave function in these trajectories never detaches, as verified by the overlap parameter in Fig. 4C, and immediately snaps back onto the sodium core upon non-adiabatic relaxation.

***Non-detachment with Delayed Relaxation*:** This second type of non-detachment behavior, illustrated in Figure 5, occurs 30% of the time. Here, instead of an immediate relaxation after the transition to the ground state, there is a lag time of ~25 fs, roughly equivalent to the inertial response of water,[43] before the spherical equilibrium ground state is reformed. During this lag time, the ground and excited-state energies remain close, and they rapidly separate to their equilibrium values only after a time delay. This lag time is correlated with the instantaneous motion of the Na-e^-_{com} distance of the (unoccupied) ground state at the instant of the transition: in this class of runs, the ground-state e^-_{com} (Fig. 5B) happens to be fluctuating away from the sodium core at the time of the transition. In the non-detachment with immediate relaxation trajectory described previously, the ground-state e^-_{com} was moving toward the core (Fig. 4B). Although this distinction may seem trivial, we will argue below that the relative motion between the Na core and the e^-_{com} of the unoccupied ground state immediately preceding the transition forms a necessary (but not sufficient) condition for electron detachment.

***Electron Detachment Trajectories*:** The next two types of trajectories, illustrated in Figures 6 and 7, show full detachment of the electron from the sodium core after the non-adiabatic transition to the ground state. In all of the detachment trajectories, the e^-_{com} of the unoccupied ground state is moving away from the sodium core at the time of the transition. Unlike the previous non-detachment cases, however, more than 98% of the charge density is at least 2.8 Å away from the

sodium after the transition (Figures 6C and 7C). The I_{max}/I_{min} (Figures 6D and 7D) shows that the electron is essentially spherical while it is detached. Thus, based on this and the similarity of the energetics to those of the hydrated electron, we can reasonably assign this species as a detached hydrated electron localized in contact with the sodium core: a contact pair. In fact, the existence of such contact pairs, defined as an electron that is separated by at most one solvent molecule from the atom, has been inferred from sub-picosecond spectroscopic experiments on both iodide[2] and sodide.[15,16] For each detachment trajectory, some time after detachment, a 'tendril' of charge density, created through solvent fluctuations, finds the sodium core with its additional stabilizing potential, promoting rapid reattachment of the electron. This tendril formation is most easily visualized in the behavior of I_{max}/I_{min} in Figs. 6D and 7D. After the transition to the ground state, the detached electron is essentially spherical, but at some point there is a large spike in I_{max}/I_{min}, indicating that the electron has become significantly aspherical. This tendril formation is followed by a rapid shift of the electron density onto the sodium. Once this occurs, the system quickly returns to equilibrium.

We can further classify the detachment trajectories into two different categories distinguished by the duration of the detachment. In the case of *short-lifetime detachment* (Fig. 6), the separation time is approximately 25 fs, a behavior seen in four (7%) of the runs. We also found four additional trajectories that met our criteria for *long-lifetime detachment* (Fig. 7), classified as any trajectory in which the detachment persisted for longer than 75 fs. The long-lifetime category included two trajectories in which detachment lasted for a picosecond or longer. Thus, while our taxonomy of the fully charge separated runs might be altered by the choice of time of separation, it is clear that there are two distinct time scales for the duration of electron detachment. These two

different time scales are in line with ideas from the experimental work on CTTS concerning solvent-separated contact pairs.[2,15,16]

To corroborate our picture of detachment, we have plotted[44] in Figure 11 the electronic charge density at different times after excitation for the short-time detachment trajectory shown in Figure 6. For each snapshot, the sodium core, shown in yellow, has the diameter of the L-J Na-O σ parameter used in the calculations. Two different electron density contours are shown: the more opaque white is the contour at 50% of the maximum charge density, which is surrounded by the semi-transparent 10% contour shown in blue. The first snapshot, labeled 0 fs, is the equilbrium configuration that marks the beginning of the trajectory. Upon excitation, which in this run occurs at 10 fs, the wave function becomes *p*-shaped; the wave function's shape is essentially unchanged at 20 fs. During the next several hundred femtoseconds nodal migration occurs, resulting in one of the lobes gradually extending into the solvent. By 750 fs the nodal migration is essentially complete, and there exists a metastable excited state until 1430 fs. These snapshots demonstrate that there is still significant electron density on the sodium after the solvent has stabilized the excited state. For this trajectory, the transition to the ground state occurs at 1435 fs, which can be seen in the loss of the node. By 1440 fs, the solvent motions have caused detachment, pulling the electron off the sodium. About 30 fs later, at 1465 fs, the solvated electron reaches a tendril toward the sodium core and its attractive potential. After finding the core, the electron rapidly moves back onto the sodium, and the newly-formed sodide then quickly relaxes to equilibrium.

To summarize our non-adiabatic simulations, we have seen that the Na^- CTTS excited state is essentially *p*-shaped. During excited-state solvation, the node of the wave function moves off the core to allow solvent to move into the nodal region. The solvent-stabilized excited state is

metastable, with electron density both on the core and protruding into an adjacent cavity in the solvent. The presence of solvent in the node causes the unoccupied ground state to increase in energy, thus serving to close the ground-to-excited-state gap. This Stokes shift is large enough to allow sufficient coupling for a non-adiabatic transition to the ground state (*cf*. Eq. 3b). Electron detachment occurs in only ~14% of the trajectories, and detachment depends on the solvent motions at the instant of the transition. But most importantly, we find that internal conversion is the most probable relaxation mechanism and that electron detachment is not necessary for relaxation to the ground state.

IV. Discussion

A. The Relationship Between the Solvation Energy Gap and Survival Probability

We can use the behavior of the trajectories to explain the shape of the survival probability curve shown in Fig. 3. The shelf in the survival probability curve at early times results from the inability of the solvent to non-adiabatically couple the ground and excited states when the ground-to-excited state energy gap is large. This is because the non-adiabatic coupling vector (Eq. 3b) includes two terms, one relating how nuclear motions mix eigenstates together, and another that is inversely proportional to the magnitude of the gap. Initially, the gap is enormous, ~4.4 eV, leaving little possibility of making a non-adiabatic transition regardless of advantageous nuclear coupling. However, as the solvent responds to the excited state and the gap closes, the energy denominator no longer dominates and the probability to make a transition becomes an interplay between the magnitude of the coupling and the size of the gap. From these considerations, we can see why there is a much smaller shelf in the hydrated electron survival probability:[20] the hydrated electron's initial

energy gap is much smaller than that of Na^- because the hydrated electron does not interact with an attractive sodium core. Though survival probability curves were not shown in any of the previous simulation work on CTTS,[6–9] we expect the basic shape of the survival probability in Fig. 3 to hold in any CTTS system that requires a substantial Stokes shift.

B. Conditions and Branching Ratios for CTTS Detachment

One of the most important questions arising from the various behaviors after the non-adiabatic transition is what determines the final behavior of the system. Do the early time dynamics after excitation affect whether the electron reattaches or not? Our results suggest that the state to which the system was initially excited plays essentially no role; in addition. neither the time required nor the extent of the nodal migration appears to determine the detachment behavior. Furthermore, we see no correlation between the excited-state lifetime and the occurrence of electron detachment. This is consistent with the metastability of the solvated CTTS excited state: memory of the initially prepared Franck-Condon CTTS state is largely forgotten.

The single characteristic that appears to correlate most strongly to detachment behavior is whether the e^-_{com} of the unoccupied ground state is fluctuating towards or away from the sodium core immediately before the transition. If the e^-_{com} of the unoccupied ground state is approaching the Na core when the nonadiabatic transition occurs, then the system immediately begins to relax to equilibrium after the transition, producing solvated sodide. However, if the e^-_{com} of the unoccupied ground state is fluctuating away from the Na core at the instant of transition, then there is a time lag (which may or may not result in detachment) before the relaxation to equilibrium occurs. For our set of trajectories, in ~86% of the runs the electron never detaches; even for trajectories in which the

Na–e^-_{com} distance was increasing at the time of the transition, there still was only a ~46% probability of detachment. Thus, we have found that a necessary (but not sufficient) condition for detachment is that the distance between the sodium atom and the e^-_{com} for the unoccupied ground state is increasing at the time of transition. Since the excited state is essentially equilibrated by the time non-adiabatic relaxation becomes possible, we expect that the direction of the Na–e^-_{com} distance fluctuations should be random, consistent with the statistics presented above.

How can we interpret this physically? At the time of the transition back to the ground state, the excited state is *p*-like in shape, with one of the lobes pinned to the sodium core and the other extended out into the water. As the solvent fluctuates, the excited state responds by shifting electron density farther out into the solvent or onto the sodium core, thus shifting the electron center of mass. The non-adiabatic transition to the ground state occurs at some point during these fluctuations. This leaves the nodeless ground state with the possibility of localizing either onto the Na core or into the cavity out in the solvent. The ability of the electron to detach is evident in the similarity of the ground state energy at the time of the transition to that of the hydrated electron (~ –2.7 eV).[19–21] Thus, depending on how the solvent is fluctuating at the time of the transition, it is possible for the electron to temporarily localize into the solvent. However, the extra stabilization from the attractive potential of the Na core ensures that the lowest-energy ground state eventually will be centered on the sodium. Indeed, the electron ultimately recombines to produce sodide in 100% of our trajectories. A heuristic interpretation is that the unoccupied ground state exists as a linear combination of a sodide-like state and a solvated electron state. When the energy of the unoccupied ground state is near that of the hydrated electron, both sodide-like and hydrated electron-like states contribute significantly, and solvent fluctuations dynamically alter the relative weights of the two

states. At the time of the transition, if the solvent is moving such that the weight of the solvated electron state is higher, then there is significant probability that the electron will detach from the sodium.

C. CTTS Solvation Dynamics and Breakdown of Linear Response

In Section III.B, we discussed the solvent motions that occur after excitation and concluded that the wave function undergoes nodal migration, allowing water molecules to enter the nodal region to provide additional solvent stabilization. In this section, we compare these motions to those present at equilibrium. To do this, we examine solvent response functions that show the dynamics of solvent rearrangement due to the perturbation of CTTS excitation. The non-equilibrium solvent response function, $S(t)$, is given by:[45]

$$S(t) = \frac{\bar{U}(t) - \bar{U}(\infty)}{\bar{U}(0) - \bar{U}(\infty)} \tag{6}$$

where $U(t)$ refers to the difference between the occupied energy level and the ground state energy level at time t, with the overbar indicating an average over all non-equilibrium trajectories. $S(t)$ is normalized so that the response function starts at one and decays to zero. The non-equilibrium solvent response function for our CTTS-excited sodide simulations is shown as the gray curve in Figure 12. The increased noise at longer times is due to the fact that trajectories that make the non-adiabatic transition to the ground state are removed from the non-equilibrium ensemble. We determine $\bar{U}(\infty)$ by averaging the excited-to-ground-state energy gap after the solvent response is largely complete; in this case over all excited-state configurations more than 2 ps after excitation.

At equilibrium, the electronic structure of the sodide solute is also determined by the solvent. This leads to the question as to whether the solvent motions responsible for fluctuations at

equilibrium are the same as those that cause non-equilibrium relaxation from the excited state: in other words, whether or not the system obeys linear response.[40] The linearity of the system can be tested by determining if the equilibrium solvent response function, $C(t)$,

$$C(t) = \frac{\langle \delta U(0)\, \delta U(t) \rangle}{\langle (\delta U(0))^2 \rangle} \tag{7}$$

is equivalent to $S(t)$, where in Eq. 7 for $C(t)$, $\delta U(t)$ is the deviation of the instantaneous energy gap at time t from its equilibrium average, and the angled brackets denote an equilibrium ensemble average. Figure 12 shows clearly that $S(t)$ does not match $C(t)$, so that CTTS excitation is not in the linear regime. Thus, there are solvent motions involved in the non-equilibrium relaxation that are not present at equilibrium.

We have previously suggested that such a breakdown of linear response can result from the solvent translational motions that occur when there is a significant size change of the solute upon excitation.[46] For our sodide system, there is a net size increase between the ground and excited states upon excitation: the average radius of gyration is 1.56 ± 0.01 Å for the ground state and 3.65 ± 0.53 Å for the excited state. However, in our previous work, we found a faster decay of $C(t)$ relative to $S(t)$ for solute size increases,[46] the opposite of what is observed in Fig. 12. In reference 46, we modeled the solute electronic states classically using spherical Lennard-Jones potentials, so that the closest solvent molecules underwent a uniform radial expansion for larger excited states. For the sodide trajectories considered here, once the repulsion of the ground-state wave function is removed, the first-shell solvent molecules close to the excited-state node experience a net inward translation due to the pressure exerted by the second solvent shell. Thus, even though the excited CTTS wave function has a larger radius of gyration than the ground state wave function, the

important solvent motions that accommodate the excited state are those responding to the local decrease in size near the excited-state node. This agrees well with the results of our classical simulations, where we found that when inward solvent translational motions are required, linear response fails because the solvent never explores these inner regions at equilibrium, leading to an $S(t)$ with a slower relaxation than $C(t)$,[46] just as observed for aqueous sodide in Figure 12. Thus, the behavior of the solvent response functions fits well with the picture we have presented for the sodide CTTS process: translational motions of first-shell solvent molecules into the excited-state node drive the relaxation of the energy gap, but these non-equilibrium motions are slower than those at equilibrium since the electron must move off the sodium core before the solvent molecules can enter into the node.

D. The Role of Symmetry in the CTTS Dynamics of Iodide versus Sodide

The principal question that we address in this work is the effect of changing the symmetry of the electronic states in CTTS systems. The change in symmetry leads to the many differences in the CTTS dynamics of aqueous sodide relative to those of iodide. First, while detachment from I^- occurs only from the lowest CTTS excited state,[6-8] detachment from Na^- occurs only after a non-adiabatic transition to the ground state. Second, while the detachment probability was unity for iodide,[8] we found only a ~20% chance of detachment from sodide. Third, we have seen that the specific solvent fluctuations at the time of the transition are critical in determining the detachment dynamics of sodide, whereas the adiabatic detachment from iodide does not seem to require any specific excited-state solvent motions, with essentially instantaneous initiation of one-photon detachment.

However disparate the CTTS detachment process may be, the relaxation to the ground state for both Na^- and I^- requires solvent motions to close the energy gap to allow for sufficient non-adiabatic coupling to return to the ground state. For both I^- and Na^-, this relaxation of the gap results primarily from destabilization of the unoccupied ground state. For sodide, it is the presence of solvent molecules in the node of the metastable *p*-like excited state that destabilizes the spherical ground state and causes the gap to close. For iodide, however, the solvation structure for the ground and undetached CTTS excited state are not radically different since both are quasi-spherical. Thus, the excited-state solvent relaxation of iodide does not sufficiently to destabilize the ground state to allow for strong non-adiabatic coupling between the ground and excited states. However, if the excited electron detaches from the iodine core, then the solvent can respond by creating both a solvated iodine atom and a solvated electron. The iodide simulations show that electron detachment incurs no significant energy penalty (i.e. the energy of the occupied excited state doesn't really change) but does have a dramatic effect on the unoccupied ground state energy (*cf.* Figure 2, Ref. 7). Thus, for the case of CTTS with the symmetry of iodide, detachment is *required* for relaxation.

In contrast, for the case of CTTS with the symmetry of sodide, the shape of the wave function allows the electron to remain attached in the excited state while providing a mechanism for solvation to sufficiently narrow the gap. The above arguments lead us to the conclusion that CTTS detachment in the Na^- system is simply a statistical event, because there exist two solvent cavities with similar energies at the time of the relaxation to the ground state. At the time of the transition, the excited-state wave function can explore either the cavity localized on the atomic core or the cavity separated from that core, allowing the electron to completely detach. In the latter case, as soon as the electron finds the core, with its extra stabilization, the newly-formed sodide rapidly

relaxes to equilibrium. Interestingly, if one were to blindly look at a solvent configuration for detached iodide, it would have a similar geometry to excited sodide: two holes in the solvent with a 'node' between them.

Thus, while altering the symmetry of the system has an important effect on the nature of the electron detachment in CTTS, the relaxation mechanism – the closing of the ground-to-excited state gap via excited-state solvation – appears to be the same for both the halides and the alkali metal anions. Moreover, the Stokes shift is also seen to be a critical step for the relaxation of the hydrated electron,[20] which has a symmetry similar to that of Na^- but lacks a nearby attractive solute. The picture presented above ties together the photoexcitation dynamics of the halides, sodide, and the hydrated electron, despite their outwardly apparent differences.

E. The Role of the Atomic Core in CTTS Dynamics

The atomic core serves two principal functions in the Na^- CTTS process: maintaining a cavity in the solvent (which will support the excited CTTS wave functions), and providing an attractive potential for the electron that alters the electronic structure relative to that of a solvated electron. Since a solvated electron will maintain it own cavity, the fundamental issue is the extent to which the potential exerted by the core alters the electronic relaxation dynamics. To better elucidate the role of the core in the CTTS dynamics of Na^-, we ran 15 non-equilibrium trajectories in which the electron-core potential (Eq. 2) was turned off completely and 15 more in which it was strengthened immediately after excitation.

1. Excited-State Dynamics with no Interaction with the Core: When the electron-core potential is turned off at the instant of excitation there is a corresponding instantaneous

destabilization of all of the electronic eigenenergies. Since the original potential interacted more strongly with eigenstates that had larger overlap with the core, when the core potential is shut off the *s*-like ground state is destabilized more than the *p*-like CTTS states, resulting in a narrowing of the gap. In the modified system without the core potential, the excited-state electron now interacts solely with water, and indeed the eigenstates of this altered system are almost identical to those of the hydrated electron.[19–22] Moreover, the dynamical behavior of the system when the excited electron-core potential is shut off also closely resembles that of the hydrated electron: there is a rapid Stokes shift that results in a non-adiabatic transition to the ground state on the few-hundred femtosecond time scale.[19,20] Thus, the altered Na^- with no core potential behaves much more like the shorter-lived hydrated electron than what we observed above for CTTS transitions.

Unlike the trajectories with the full potential, the electron with the modified potential invariably returns to the cavity containing the atomic core on transition to the ground state. Why would the electron prefer to localize in the atomic cavity rather than the cavity made from the extended lobe? One answer could be that because of the decreased energy gap and correspondingly faster non-adiabatic relaxation, the electron that interacts with the modified potential never has time to fully form two equivalent cavities. Even if there were enough time, however, we would still expect the electron to favor the cavity containing the core. This is because upon transition to the ground state, the now nodeless electron is still subject to solvent fluctuations. However, the cavity that contains the core will be more resistant to fluctuations due to solvent-core repulsions; thus, the effect of fluctuations on the electron lobes is not symmetric, causing the part of the ground-state electron that was extended into the solvent to be shoved into the cavity being maintained by the atomic core. This suggests that the presence of the classical core in a solvent cavity could drive

reattachment of the electron simply due to the fact that the classical core makes one cavity more stable.

2. Excited-state Dynamics with Increased Interaction with the Core: In addition to trajectories in which the electron-core potential was removed upon excitation, we also ran trajectories in which the electron-core potential was strengthened[47] at the instant of excitation. We chose the new electron-core potential so as not introduce any additional bound eigenstates (to prevent access to new relaxation channels); thus, the deepest new potential we could create lowered the ground state energy to approximately –9 eV. As above, changing the core potential affects the different eigenstates in different ways. Deepening the potential well of the Na core causes the ground state to be lowered more than the three *p*-like CTTS states, thus increasing the ground-to-first-excited-state energy gap. With this increased gap, the excited-state solvent reorganization is not sufficient to bring the ground and occupied excited eigenstates close in energy. Thus, there is a much smaller probability for non-adiabatic relaxation, leading to accordingly longer lifetimes (12.3 ps vs. 1.2 ps in section III.B). Since the solvent reorganization energy is not sufficient to close the gap, we might expect the excited-state electron to detach, as is the case for I^-. However, for adiabatic electron detachment to occur, the energy level of the occupied excited state must be equal to (or higher) than that of the solvated electron, as is the case for I^-. With the deepened core potential, the lowest excited Na^- state is well below the energy of the (detached) solvated electron, leaving no driving force for detachment.

As also might be expected, these simulations with the deepened electron-Na core interaction do not show significant migration of the node in the excited state. This result is consistent with our arguments in Sec. III.B, where we suggested that nodal migration results from a competition

between the stabilization of the electron by the attractive core potential and stabilization of the electron by solvation as solvent molecules move into the nodal region. In the deepened-core trajectories, the loss of wave function overlap with the core that would occur during nodal migration is greater than the lowering of the energy resulting from ideal solvation of the node; thus, the deepened core acts as a trapping center for the excited-state electron.

V. Conclusions

We have performed a series of non-adiabatic mixed quantum/classical MD simulations of the CTTS dynamics of photoexcited sodide in water. Our choice of water as the solvent has allowed us to make direct comparisons with previous simulations of both the hydrated electron and the CTTS dynamics of the aqueous halides. We find that changing the symmetry of the CTTS electronic states has a strong effect on system behavior, altering the way in which the solvent promotes electron detachment. For sodide, with its *s*-like ground state and 3 *p*-like CTTS excited states, CTTS excitation leads to nodal migration, with one lobe extended out into the solvent and the other pinned to the Na core. This migration occurs so that solvent molecules, which would otherwise be blocked by the sodium core, can stabilize the excited state by moving into the nodal region. These solvent motions into the nodal region also result in a breakdown of linear response. Furthermore, simulations with altered electron-core potentials show that nodal migration is a competitive process between excited-state solvation and reduction of the overlap of the electron with the attractive potential of the core. Unlike the haldies, CTTS excitation of sodide in water produces a metastable excited state: detachment from sodide results only after the non-adiabatic transition to the ground state. Moreover, unlike the unit detachment yield from iodide, excitation of aqueous sodide results

in detachment only ~20% of the time, dependent on the specific solvent motions taking place at the instant of the non-adiabatic transition.

By comparing our simulations to previous work on the aqueous halides, we proposed a picture for CTTS relaxation in systems with any electronic symmetry. After excitation, a substantial Stokes shift is required to close the large ground-to-excited-state energy gap and provide for sufficient non-adiabatic coupling to allow the transition back to the ground state. In all the CTTS simulations that we are aware of, this results from destabilization of the ground state due to excited-state solvation, which closes the gap by producing an unfavorable solvation structure for the unoccupied ground state. For sodide, nodal migration of the excited state is sufficient to produce the necessary Stokes shift. But for CTTS excitation of the halides, the similarity of the excited-state and ground-state solvation structures prior to detachment dictates that electron separation take place from the excited state. It is only after detachment, which is an essentially energetically neutral process for the CTTS excited states of halides, that solvation can produce the necessary Stokes shift to allow for a non-adiabatic transition back to the ground state. Thus, one critical result of the change in symmetry between iodide and sodide is that detachment is not a possible relaxation pathway for CTTS-excited sodide: there is simply no way for the excited *p*-like CTTS state to detach into an *s*-like solvated electron unless a non-adiabatic transition removes the node in the excited-state wavefunction. Instead, CTTS detachment from sodide, which results from the creation of a second solvent cavity by the lobe extended into the solvent during nodal migration, occurs only if solvent fluctuations at the time of the excited-to-ground-state transition prevent immediate access to the sodium core.

Finally, we comment on the connection between the simulations presented here and ultrafast

experiments studying the CTTS dynamics of sodide.[15–17] Our simulations predict that unlike iodide, there is a low detachment probability following CTTS excitation, resulting from the fact that electron detachment from sodide occurs for different physical reasons than electron detachment from iodide. Yet, the Na^- experiments have not indicated that the detachment quantum yield is significantly less than unity.[15–17] This discrepancy between the Na^- simulations and experiments has two possible explanations: either internal conversion is faster than the time resolution of the experiments, or the choice of solvent in our simulations radically alters the detachment probability. THF is a larger, less polar solvent than water, and its dynamics occur on fundamentally slower time scales than water. Moreover, the solvated electron in THF behaves quite differently than that in water: the THF-solvated electron's cavity supports only one bound state, and this bound state is quite a bit more delocalized than the corresponding ground state of the hydrated electron.[48] This delocalization will change the relative strengths of solvation and the overlap of the wave function with the atomic core in THF compared to water. Thus, while we expect the basic picture of 3 solvent-split excited states and nodal migration to hold for CTTS dynamics in both water and THF, there are likely to be significant changes in the dynamics following the non-adiabatic transition in the two solvents. We are presently working to repeat these simulations in THF and to examine whether the calculated spectroscopic signals match experiment. We also plan to take advantage of a newly-developed algorithm for simulating multi-electron, non-adiabatic dynamics[14] to compare one-electron and two-electron CTTS trajectories of sodide, directly illuminating the roles of exchange and correlation in the dynamics of electron transfer.

Acknowledgements: This work was supported by the National Science Foundation under grant

number CHE-0240776 and by the UCLA Council on Research. B.J.S. is a Cottrell Scholar of Research Corporation and a Camille Dreyfus Teacher-Scholar. We are grateful to Kim Wong for providing some of the code used for MF/SH, and for many helpful discussions. Computational resources for this work were provided in part by an Academic Equipment Grant from Sun Microsystems and the Bradley University Evolutionary Algorithm Group.

References:

[1] M.J. Blandamer and M.F. Fox, Chem. Rev. **70**, 59 (1970).

[2] V. H. Vilchiz, J. A. Kloepfer, A. C. Germaine, V. A. Lenchenkov, and S.E. Bradforth, J. Phys. Chem. A **105**, 1711 (2001); J. A. Kloepfer, V. H. Vilchiz, V. A. Lenchenkov, A. C. Germaine, and S. E. Bradforth, J. Chem. Phys. **113**, 6288 (2000); J. A. Kloepfer, V. H. Vilchiz, V. A. Lenchenkov, and S.E. Bradforth, Chem. Phys. Lett. **298**, 120 (1998).

[3] L. Lehr, M. T. Zanni, C. Frischkorn, R. Weinkauf, and D. M. Neumark, Science **284**, 635 (1999); A. V. Davis, M. T. Zanni, C. Frischkorn, and D. M. Neumark, J. Elec. Spec. Rel. Phen. **108**, 203 (2000); M. T. Zanni, C. Frischkorn, A. V. Davis, and D. M. Neumark, J. Phys. Chem. A **104**, 2527 (2000); A. V. Davis, M. T. Zanni, R. Weinkauf, and D. M. Neumark, Chem. Phys. Lett. **353**, 455 (2002).

[4] F. H. Long, X. Shi, H. Lu, and K.B. Eisenthal, J. Phys. Chem. **98**, 7252 (1994); F. H. Long, H. Lu, X. Shi, and K. B. Eisentahl, Chem. Phys. Lett. **169**, 165 (1990); F. H. Long, H. Lu, and K. B. Eisenthal, J. Chem. Phys. **91**, 4413 (1989).

[5] Y. Gauduel, M. Sander, H. Gelabert, J. Molec. Liq. **78**, 111 (1998); H. Gelabert and Y. Gaudel, J. Phys. Chem. **100**, 13993 (1996); Y. Gaudel, H. Gelabert, and M. Ashokkumar, Chem. Phys. **197**, 167 (1995); Y. Gauduel, H. Gelabert, and M. Ashokkumar, J. Molec. Liq. **64**, 57 (1995).

[6] W.-S. Sheu and P. J. Rossky, J. Phys. Chem. **100**, 1295 (1996).

[7] W.-S. Sheu and P. J. Rossky, Chem. Phys. Lett., **213**, 233 (1993).

[8] W.-S. Sheu and P. J. Rossky, J. Amer. Chem. Soc. **115**, 7729 (1993); W.-S. Sheu and P. J. Rossky, Chem. Phys. Lett. **202**, 186 (1993).

[9] A. Staib and D. Borgis, J. Chem. Phys. **103**, 2642 (1995); A. Staib and D. Borgis, J. Chem. Phys. **104**, 9027 (1996); A. Staib and D. Borgis, J. Chem. Phys. **104**, 4776 (1996).

[10] S. E. Bradforth and P. Jungwirth, J. Phys. Chem. A **106**, 1286 (2002)

[11] H. Y. Chen and W.-S. Sheu, J. Amer. Chem. Soc. **122**, 7534 (2000); H. Y. Chen and W.-S. Sheu,

Chem. Phys. Lett. **335**, 475 (2001); H.Y. Chen and W.-S. Sheu, Chem. Phys. Lett. **353**, 459 (2002).

[12] J. A. Kloepfer, V. H. Vilchiz, V. A. Lenchenkov, X. Chen, and S. E. Bradforth, J. Chem. Phys. **117**, 766 (2002).

[13] A. Farkas and L. Farkas, Farad. Trans. Soc. **34**, 1120 (1938); J. Jortner, R. Levine, M. Ottolenghi, and G. Stein, J. Phys. Chem. **65**, 1232 (1961); J. Jortner, M. Ottolenghi, and G. Stein, J. Phys. Chem. **66**, 2029 (1962); F. S. Dainton and S. R. Logan, Proc. R. Soc. London, Ser. A **287**, 281 (1965); G. Czapski and M. Ottolenghi, Isr. J. Chem. **6**, 75 (1968), G. Czapski, J. Ogdan, and M. Ottolenghi, Chem. Phys. Lett. **3**, 383 (1969).

[14] R. E. Larsen and B. J. Schwartz, *submitted for publication.*

[15] E. R. Barthel, I. B. Martini, and B. J. Schwartz, J. Chem. Phys. **112**, 9433 (2000); I. B. Martini, E. R. Barthel, and B. J. Schwartz, J. Chem. Phys. **113**, 11245 (2000); E. R. Barthel, I. B. Martini, and B. J. Schwartz, J. Phys. Chem. B **105**, 12230 (2001); E. R. Barthel, I. B. Martini, E. Keszei and B. J. Schwartz, J. Chem. Phys. **118**, 5916 (2003); E. R. Barthel and B. J. Schwartz, Chem. Phys. Lett., in press.

[16] I. B. Martini, E. R. Barthel, and B. J. Schwartz, J. Amer. Chem. Soc. **124**, 7622 (2002); I. B. Martini, E. R. Barthel, and B. J. Schwartz, Science **293**, 462 (2001); I. B. Martini and B. J. Schwartz, Chem. Phys. Lett. **360**, 22 (2002).

[17] Z. H. Wang, O. Shoshana, B. X. Hou and S. Ruhman, J. Phys. Chem. A **107**, 3009 (2003).

[18] See, e.g., M. J. Tauber and R. A. Mathies, J. Am. Chem. Soc. **125**, 1394 (2003); P. Kambhampati, D. H. Son, T. W. Kee and P. F. Barbara, J. Phys. Chem. **106**, 2374 (2002); A. Baltuska, M. F. Emde, M. S. Pshenchnikov and D. A. Wiersma, J. Phys. Chem. **103**, 10065 (1999).

[19] K. F. Wong and P. J. Rossky, J. Phys. Chem. A **105**, 2546 (2001); K. F. Wong and P. J. Rossky, J. Chem. Phys. **116**, 8418 (2002); K. F. Wong and P. J. Rossky, J. Chem. Phys. **116**, 8429 (2002).

[20] B. J. Schwartz and P. J. Rossky, J. Chem. Phys. **105**, 6997 (1996); B. J. Schwartz, P. J. Rossky, J.

Chem. Phys. **101**, 6902 (1994); B. J. Schwartz, P. J. Rossky, J. Chem. Phys. **101**, 6917 (1994); B. J. Schwartz and P. J. Rossky, J. Phys. Chem. **98**, 4489 (1994).

[21] J. Schnitker, K. Motakkabir, P. J. Rossky and R. A. Friesner, Phys. Rev. Lett. **60**, 456 (1988); P. J. Rossky and J. Schnitker, J. Phys. Chem. **86**, 3471 (1987); F. A. Webster, J. Schnitker, M. S. Friedrichs, R. A. Friesner and P. J. Rossky, Phys. Rev. Lett. **33**, 3172 (1991); T. H. Murphrey and P. J. Rossky, J. Chem. Phys. **99**, 515 (1993).

[22] See, e.g., L. Turi and D. Borgis, J. Chem. Phys. **117**, 6186 (2002); M. Boero, M. Parrinello, K. Terakura, T. Ikeshoji and C. C. Liew, Phys. Rev. Lett. **90**, 226403 (2003); E. Neria, A. Nitzan, R. N. Barnett and U. Landman, Phys. Rev. Lett. **67**, 1011 (1991); A. Staib and D. Borgis, J. Phys. Chem. **103**, 2642 (1995).

[23] O. V. Prezhdo and P. J. Rossky, J. Chem. Phys. **107**, 825 (1997).

[24] P. Ehrenfest, Z. Phys. **45**, 455 (1927).

[25] J. C. Tully, J. Chem. Phys. **93**, 1061 (1990).

[26] F. Webster, P. J. Rossky, and R. A. Friesner, Comp. Phys. Commun. **63**, 494 (1991).

[27] F. Webster, E. T. Wang, P. J. Rossky and R. A. Friesner, J. Chem. Phys. **100**, 4835 (1994).

[28] J. Schnitker and P. J. Rossky, J. Chem. Phys. **86**, 3462 (1987).

[29] R. W. Shaw, Jr., Phys. Rev. **174**, 769 (1968).

[30] L. Szasz, *Pseudopotential Theory of Atoms and Molecules* (Wiley, New York, 1985).

[31] P. W. Atkins, *Molecular Quantum Mechanics*, 2nd ed. (Oxford University Press, Oxford, 1983).

[32] A. M. James and M. P. Lord, *Macmillan's Chemical and Physical Data* (Macmillan, London, 1992) via http://www.webelements.com.

[33] S. Hammes-Schiffer and J. C. Tully, J. Chem. Phys. **101**, 4657 (1994).

[34] K. Toukan and A. Rahman, Phys. Rev. B **31**, 2643 (1985).

[35] M. P. Allen and D. J. Tildesely, *Computer Simulation of Liquids*, Oxford University Press: New York (1987).

[36] D. Chekmarev, M. Zhao, S.A. Rice, J. Chem. Phys. **109**, 768 (1998).

[37] J. J. Sakurai, *Modern Quantum Mechanics*, Addison-Wesley: Reading, MA (1994).

[38] A. L. Sobolewski and W. Domcke, Phys. Chem. Chem. Phys. **4**, 4 (2002); J. Kim, H. M. Lee, S. B. Suh, D. Manjumdar, K. S. Kim, J. Chem. Phys. **113**, 5249 (2000); D. Majumdar, J. Kim, K. S. Kim, J. Chem. Phys. **112**, 101 (2000); F. D. Vila and K. D. Jordan, J. Phys. Chem. A **106**, 1391 (2002).

[39] There was one run that was excited to a continuum state. This represents a rare fluctuation since the average oscillator strength for a continuum transition is two orders of magnitude smaller than the *p*-transitions; however, in this particular case, the continuum oscillator strength was 1/3 that of the CTTS transition. Regardless, the long time behavior of this trajectory is indistinguishable from the others.

[40] D. Chandler, *Introduction to Modern Statistical Mechanics* (Oxford University Press, Oxford, 1987).

[41] We take the reversible work theorem, which is well defined for a classical system, as an ansatz for our mixed QM/CM system.

[42] Using a longer-time cutoff did not have any apparent effect on the PMF beyond the introduction of additional noise due to poorer statistics.

[43] M. Maroncelli and G. R. Fleming, J. Chem. Phys. **86**, 6221 (1987).

[44] L. Laaksonen, J. Mol. Graph. **10**, 33 (1992); D. L. Bergman, L. Laaksonen, A. Laaksonen, J. Mol. Graph. Model. **15**, 310 (1997).

[45] M. Maroncelli, J. Mol. Liq. **57**, 1 (1993).

[46] D. Aherne, V. Tran, and B. J. Schwartz, J. Phys. Chem. B **104**, 5382 (2000); V. Tran and B. J. Schwartz, J. Phys. Chem. B **103**, 5570 (1999).

[47] The potential was strengthened by a constant, $V(r) \rightarrow \alpha V(r)$, but had the same functional form as Eqns. 1-2.

[48] L. Kevan, Acc. Chem. Res. **14**, 138 (1981).

Figure Captions:

Figure 1: Dynamical history of the adiabatic eigenstates for a typical 1-ps portion of the equilibrium aqueous sodide trajectory. There is a single *s*-like ground state, a band of 3 *p*-like solvent-stabilized CTTS excited states, and a set of continuum states (of which the lowest two are shown).

Figure 2: The density of states for the equilibrium electronic structure of aqueous sodide. Each peak represents the distribution of adiabatic energies for the ground state, the three bound excited states, and a single continuum state. The arrow connecting the ground state and first excited state peaks corresponds to the energy gap used to select the initial configurations for the non-equilibrium trajectories.

Figure 3: Excited-state survival probability for CTTS-excited aqueous sodide as a function of time for the 54 non-adiabatic trajectories.

Figure 4: Information for a typical trajectory for the non-detachment pathway; this type of trajectory occurred 56% of the time. **(A)** Dynamical history of the lowest six adiabatic energy levels of sodide for a non-adiabatic trajectory with CTTS excitation. The gray-shaded line indicates the occupied electronic state. The arrow indicates the time of the non-adiabatic transition from the excited state to the ground state. **(B)** The distance between the sodium atom and the center-of-mass of the electron for the ground and first excited states as a function of time. The gray-shaded line indicates the occupied state. **(C)** The overlap parameter, Z, (Eq. 4 with r_c = 2.8 Å) as a function of time for the occupied state. **(D)** The ratio of the largest to the smallest moment of inertia for the charge density of the occupied electronic state as a function of time.

Figure 5: Information for a typical trajectory for the delayed non-detachment pathway. This type of trajectory, which occurred 30% of the time, differs from those represented by Fig. 4 in that there is a lag time (~25 fs) after the transition to the ground state before the energy levels relax to their equilibrium values. Panels **A-D** provide the same information for this trajectory as in Fig. 4.

Figure 6: Information for a typical trajectory for the short-time detachment pathway. In this class of trajectories, which occurred 7% of the time, the electron detaches for a short period of time (< 75 fs). Panels **A-D** provide the same information for this trajectory as in Fig. 4.

Figure 7: Information for a typical trajectory for the long-time detachment pathway. In this class of trajectories, which occurred 7% of the time, the electron detaches for a long period of time (> 75 fs). This class includes two trajectories where the electron remained detached for a picosecond or longer. Panels **A-D** provide the same information for this trajectory as in Fig. 4.

Figure 8: Potential of mean force (PMF) for the interaction of the excited-state electron with the Na core. The top panel shows the PMF assuming that the wave function-sodium relative orientation is constrained to a line in space (Eq. 5a); the bottom panel shows the PMF assuming that the electron and sodium atom explore all relative orientations (Eq. 5b). See the text for details. The error bars are one standard deviation.

Figure 9: Na atom/solvent site radial distribution functions, $g(r)$, for the equilibrated ground (black curves) and excited states (grey curves). The upper panel shows the Na-O pair distribution, and the lower panel shows the Na-H pair distribution. The excited-state distributions were computed by

averaging over nonequilibrium solvent configurations that were more than 450 fs after the excitation.

Figure 10: Electron center-of-mass/solvent site radial distribution functions, $g(r)$, for the equilibrated ground (black curves) and excited states (grey curves). The upper panel shows the e^--O pair distribution, and the lower panel shows the e^--H pair distribution. The excited-state distributions were computed by averaging over nonequilibrium solvent configurations that were more than 450 fs after the excitation. The noise at small distances in the e^--H distribution is the result of poor statistics, since few H atoms approach this close to the electron's center of mass.

Figure 11: Time evolution of the electron density of CTTS-excited sodide for the short-time detachment trajectory detailed in Fig. 6. The neutral sodium atom is shown as a 3.2 Å-diameter yellow sphere. The wave function in each snapshot is the electronic density of the occupied state at the labeled time step: the more opaque white denotes the 50% charge density contour and the light blue indicates the 10% contour. Although (for presentation purposes) some snapshots have been rotated a small amount, the overall orientation of the lobes is accurately represented (i.e. lying horizontally in the figure). The time of excitation for this run was 10 fs; therefore, for example, the 1440-fs snapshot shows the system 1430 fs after excitation.

Figure 12: The equilibrium response function, $C(t)$, (Eq. 7, black curve) and the non-equilibrium response function, $S(t)$, (Eq. 6, gray curve) for CTTS excitation of aqueous sodide.

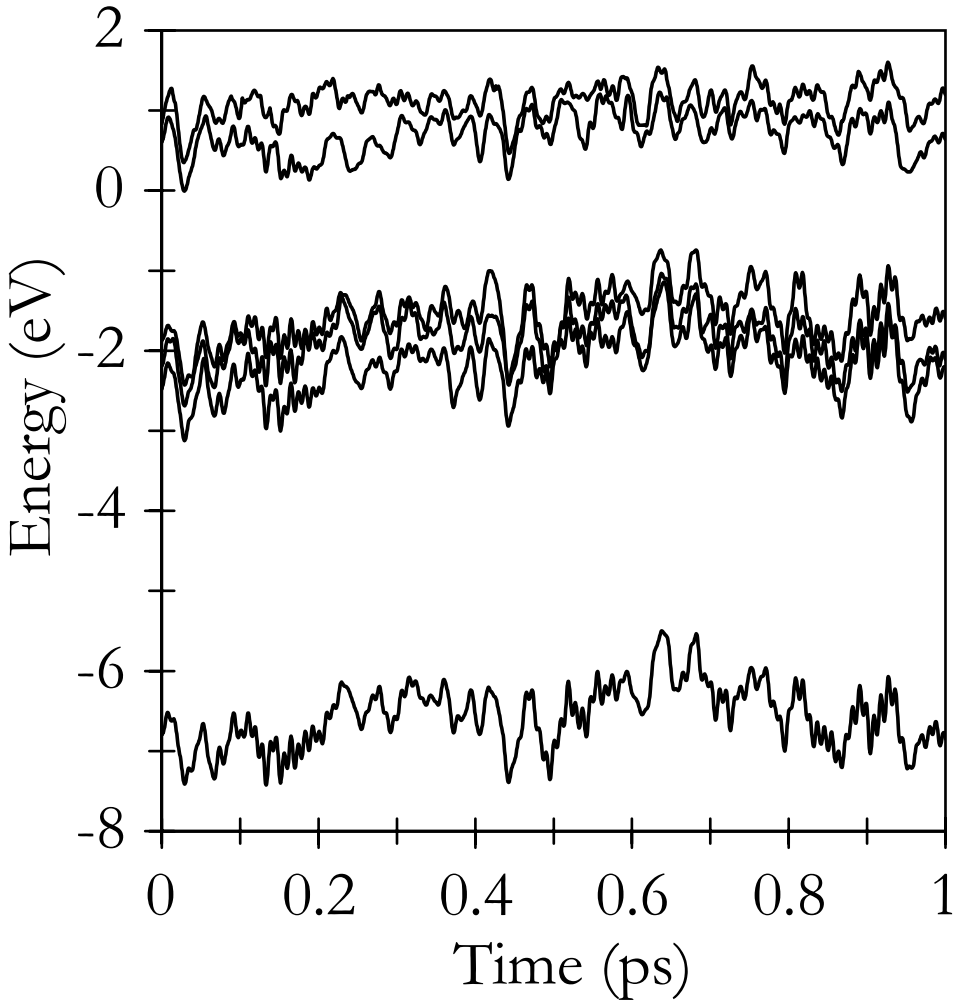

Smallwood, et. al. Figure 1

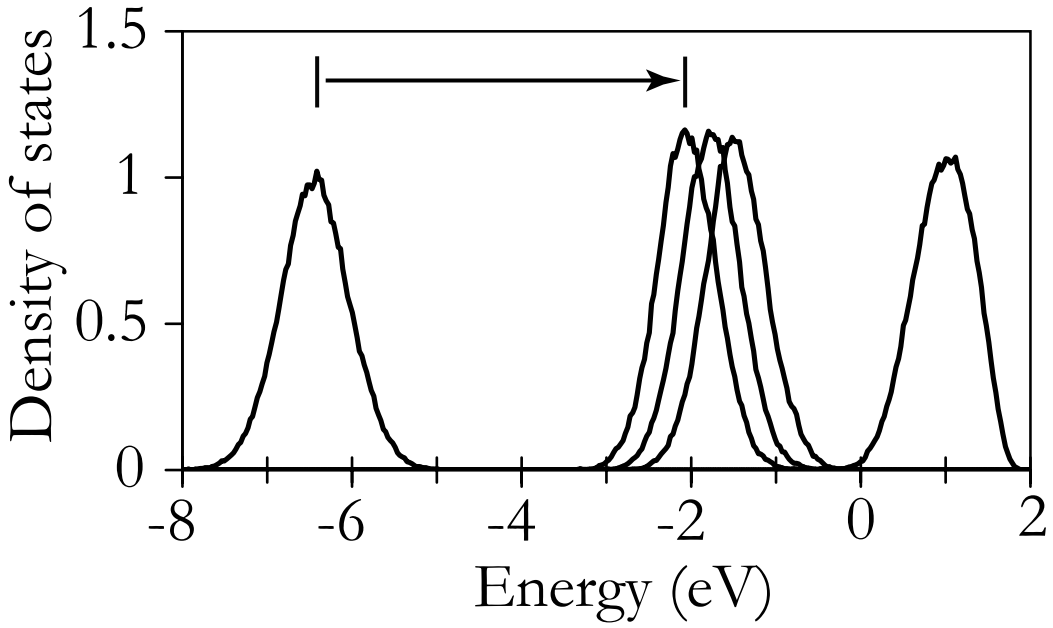

Smallwood, et. al. Figure 2

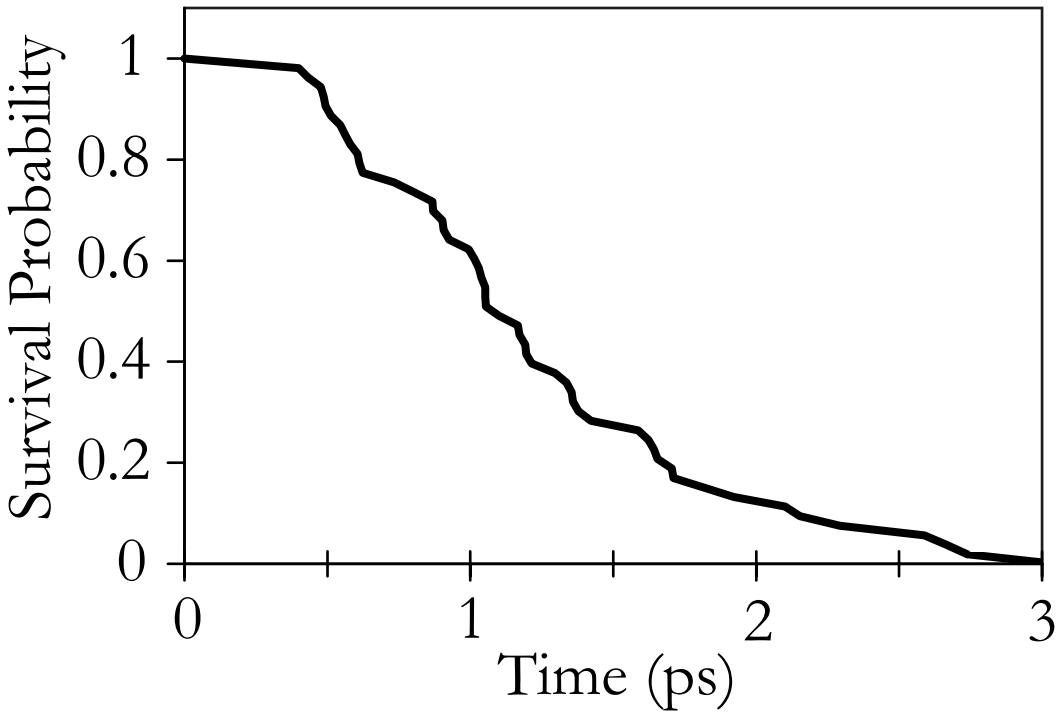

Smallwood, et. al. Figure 3

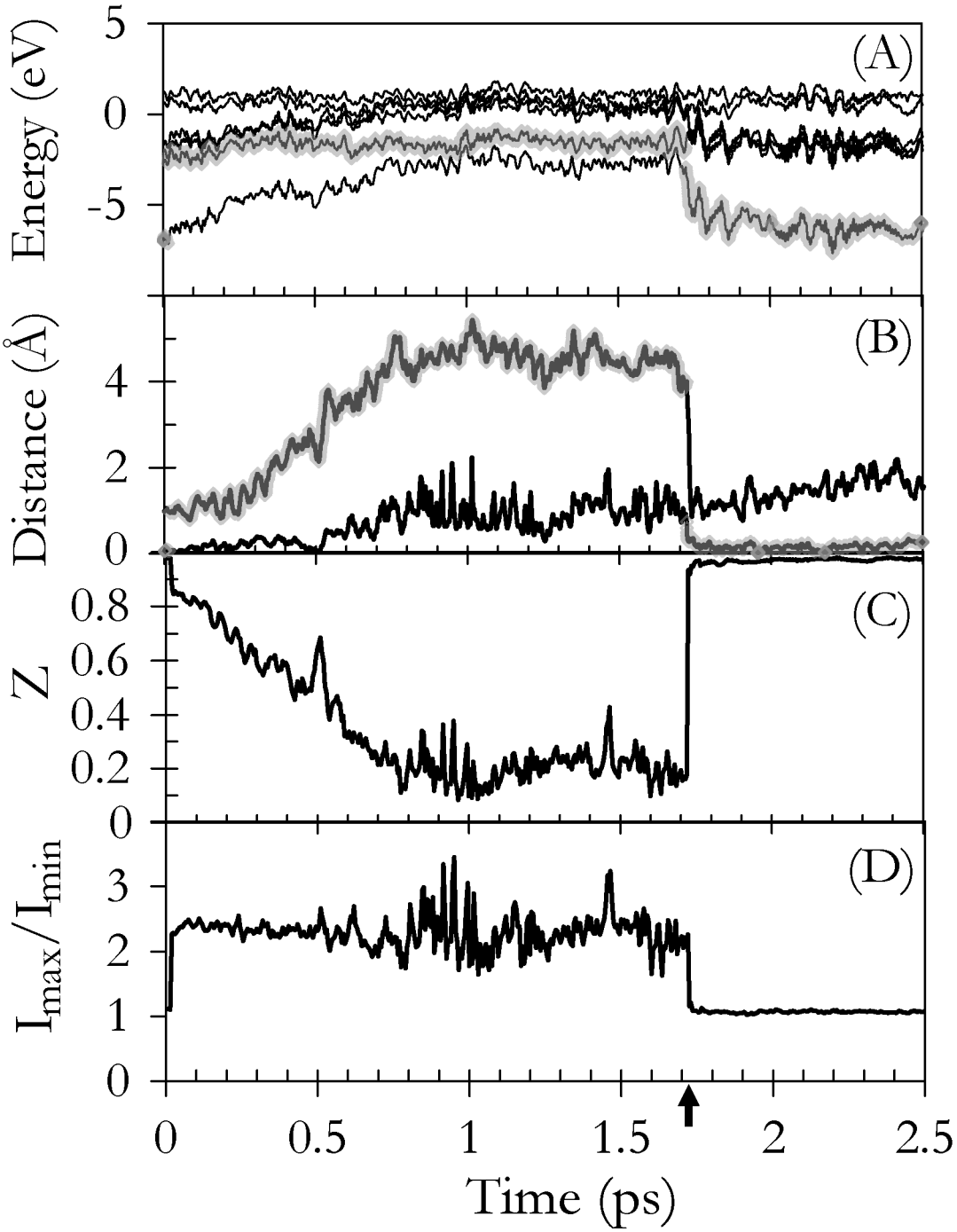

Smallwood, et. al., Figure 4

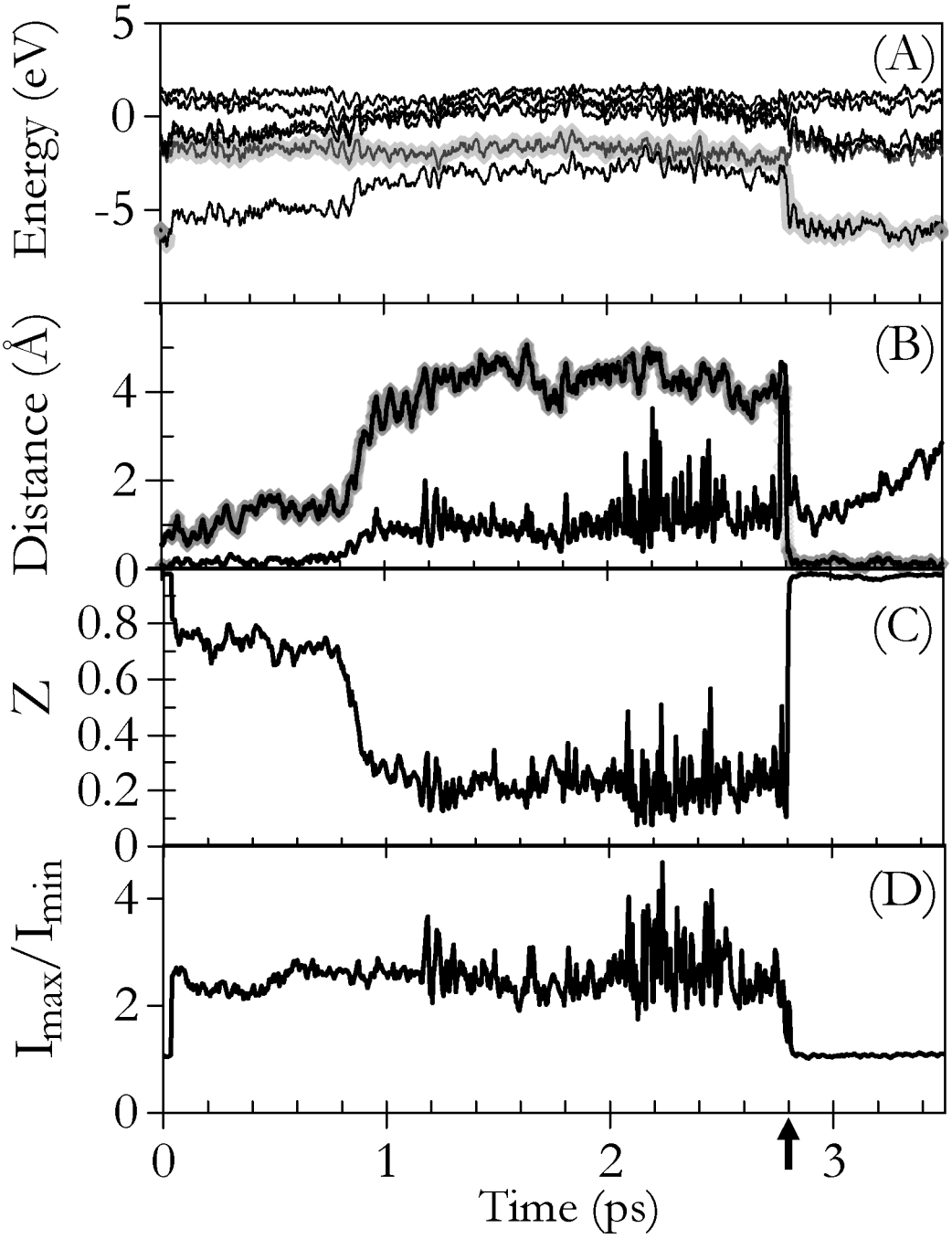

Smallwood, et. al. Figure 5

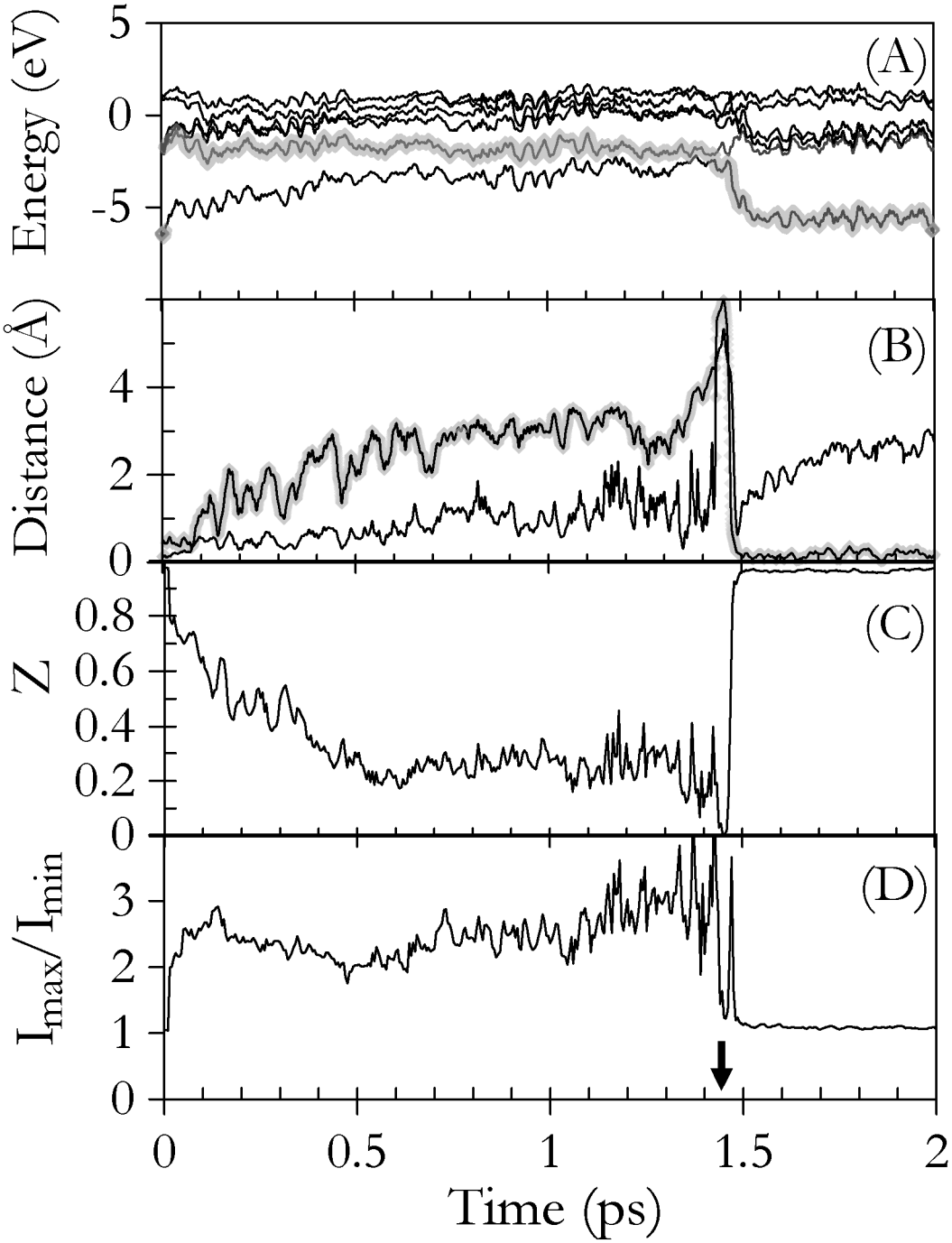

Smallwood, et. al., Figure 6

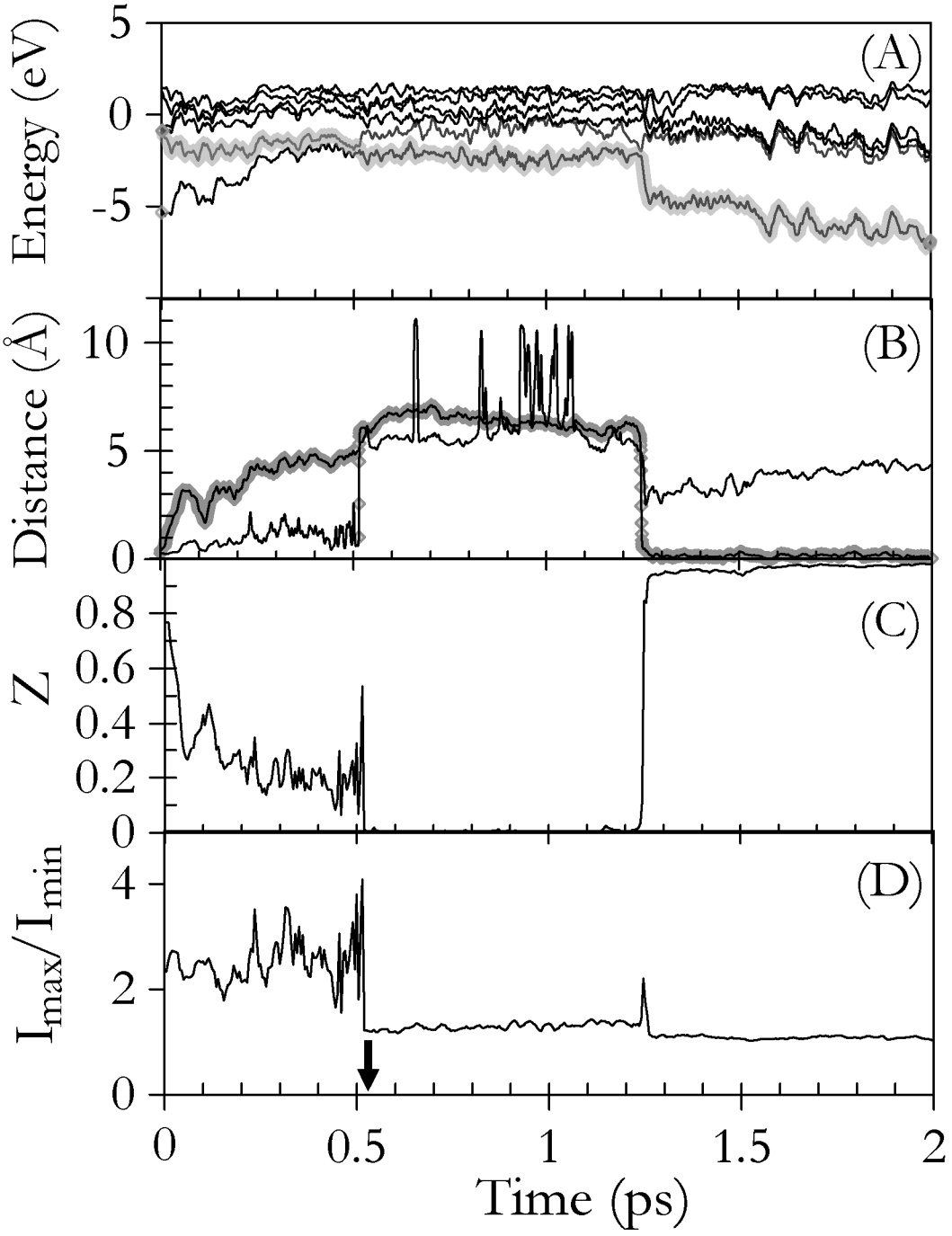

Smallwood, et. al., Figure 7

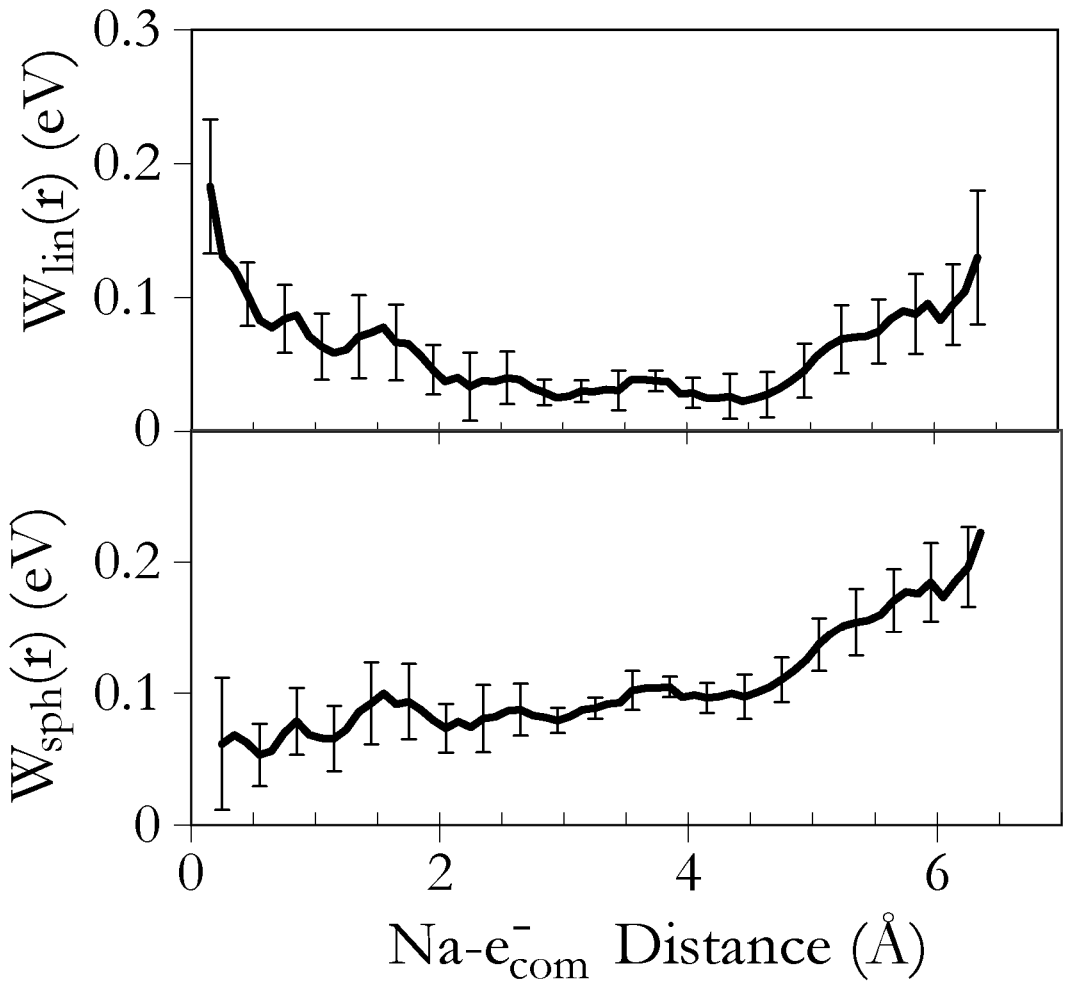

Smallwood et al., Figure 8

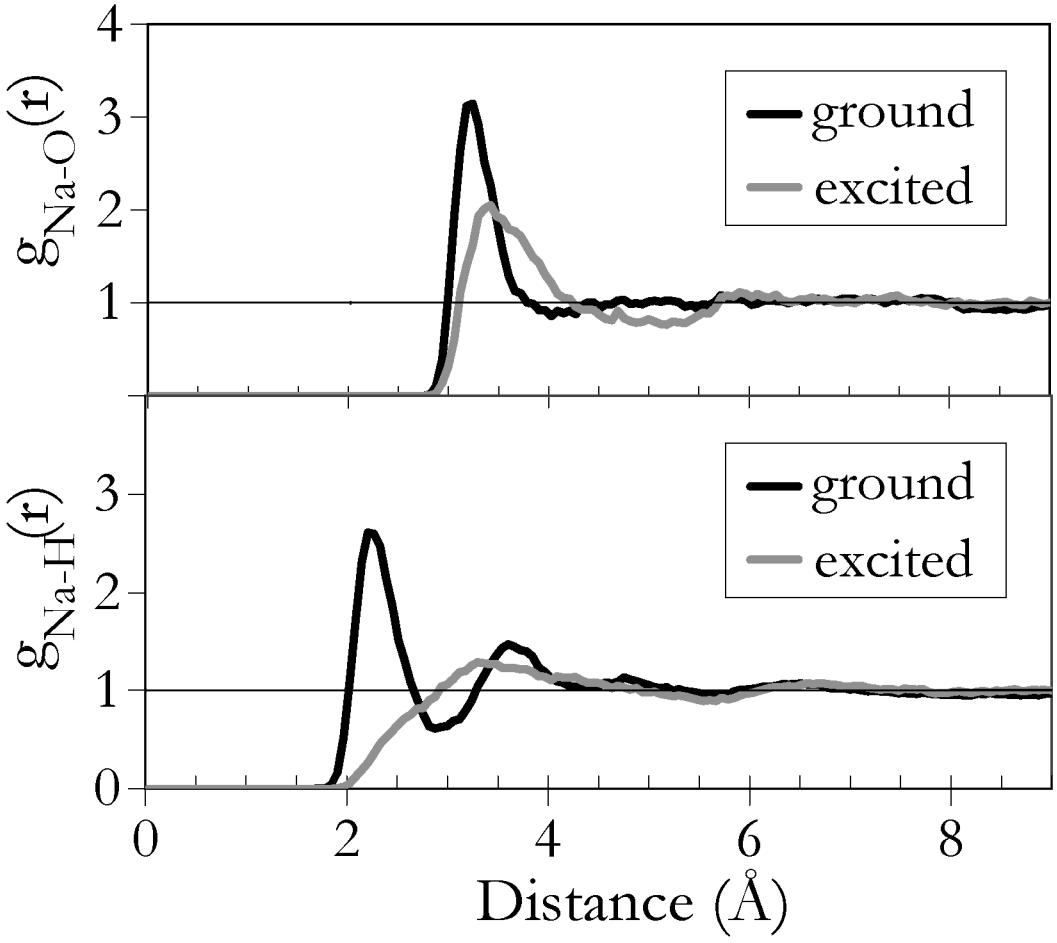

Smallwood et al., Figure 9

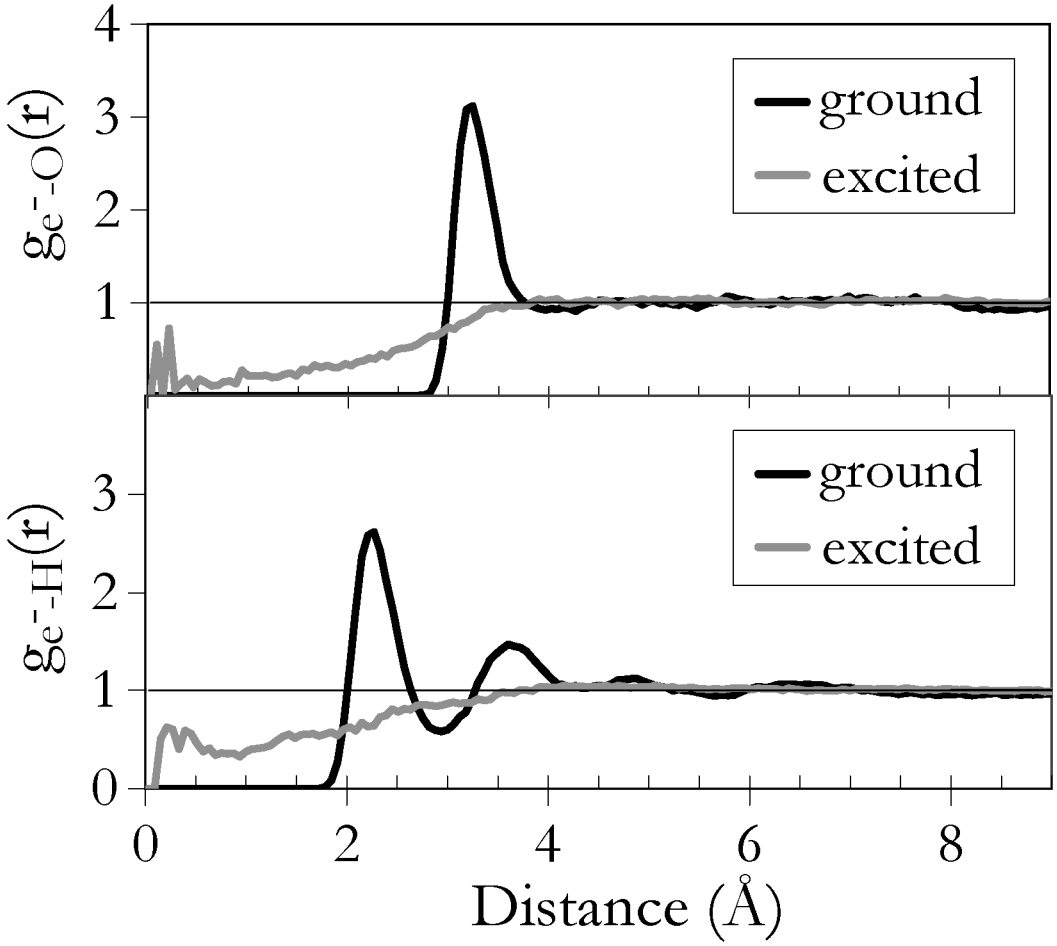

Smallwood et al., Figure 10

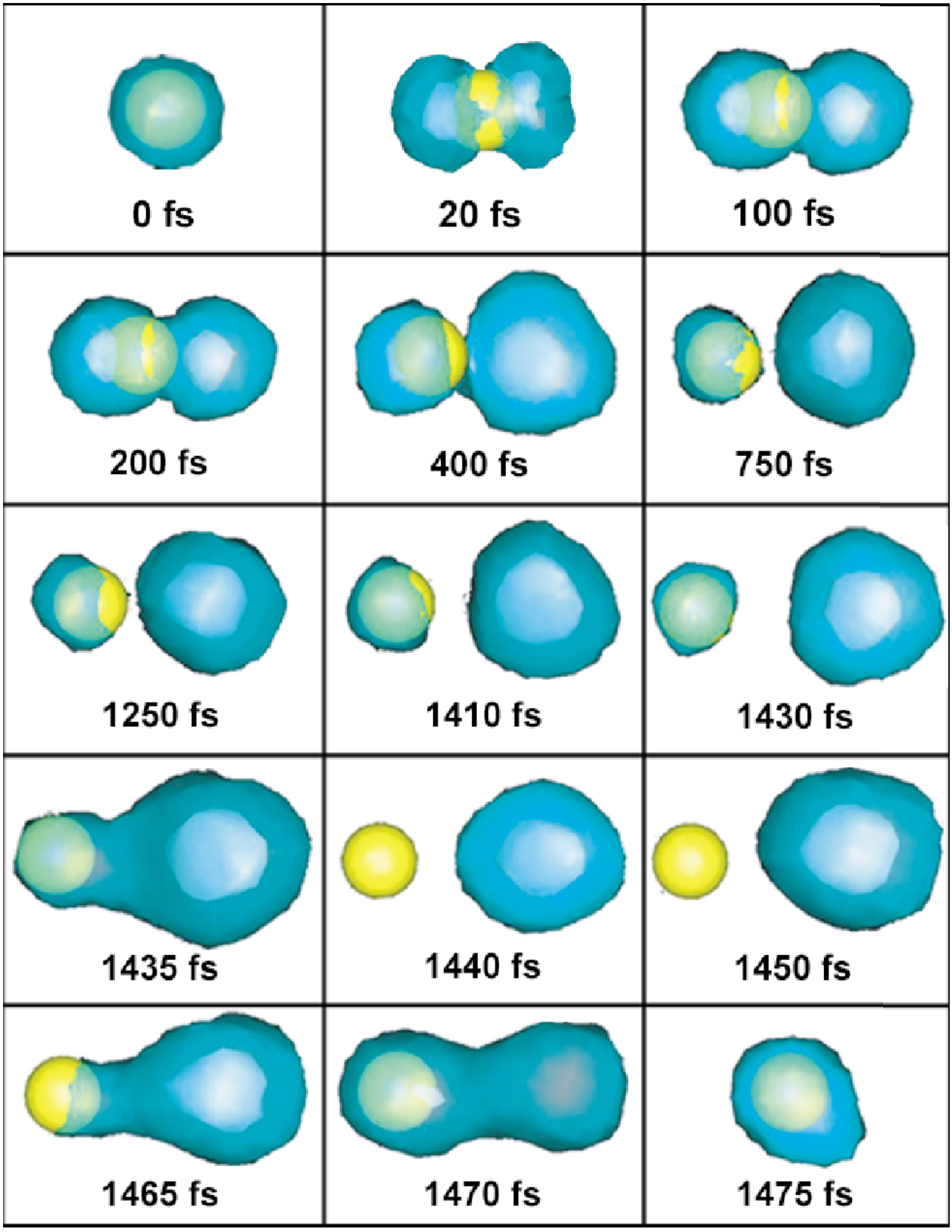

Smallwood, et al., Figure 11

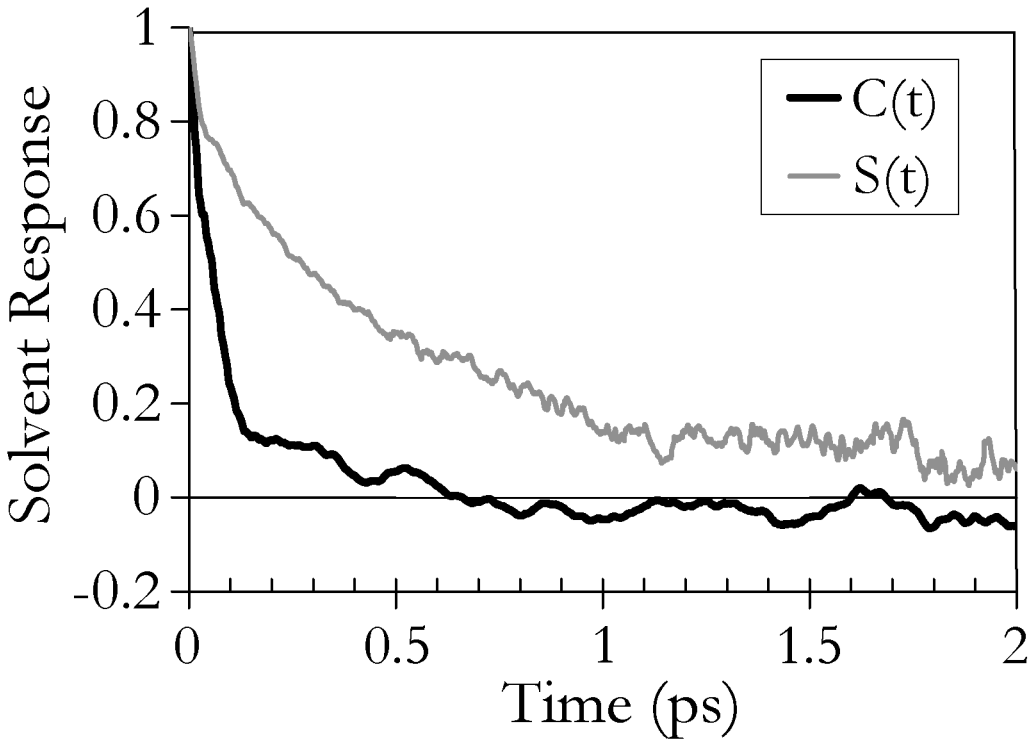

Smallwood, et. al., FIgure 12